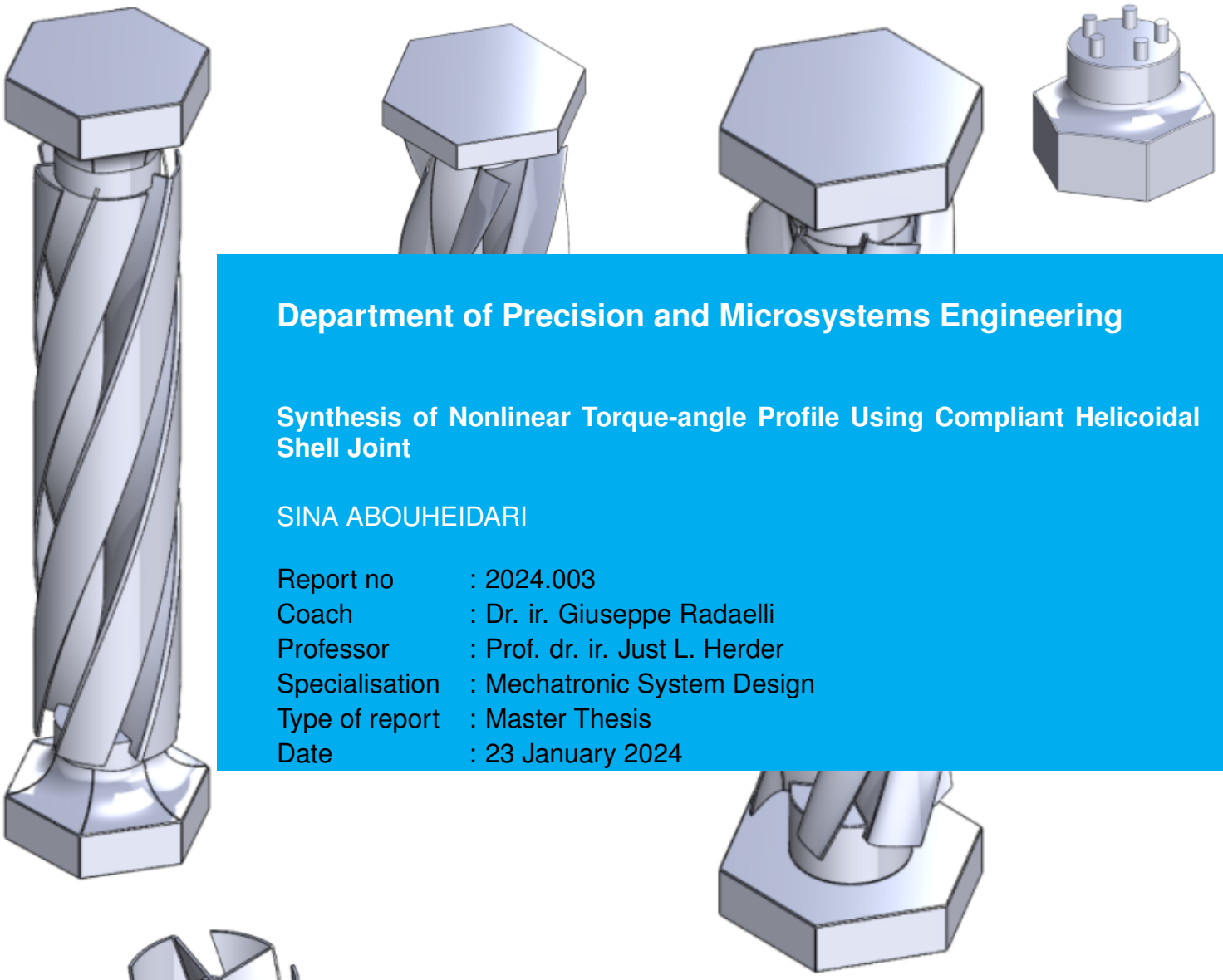

Department of Precision and Microsystems Engineering

Synthesis of Nonlinear Torque-angle Profile Using Compliant Helicoidal Shell Joint

SINA ABOUHEIDARI

Report no : 2024.003
Coach : Dr. ir. Giuseppe Radaelli
Professor : Prof. dr. ir. Just L. Herder
Specialisation : Mechatronic System Design
Type of report : Master Thesis
Date : 23 January 2024

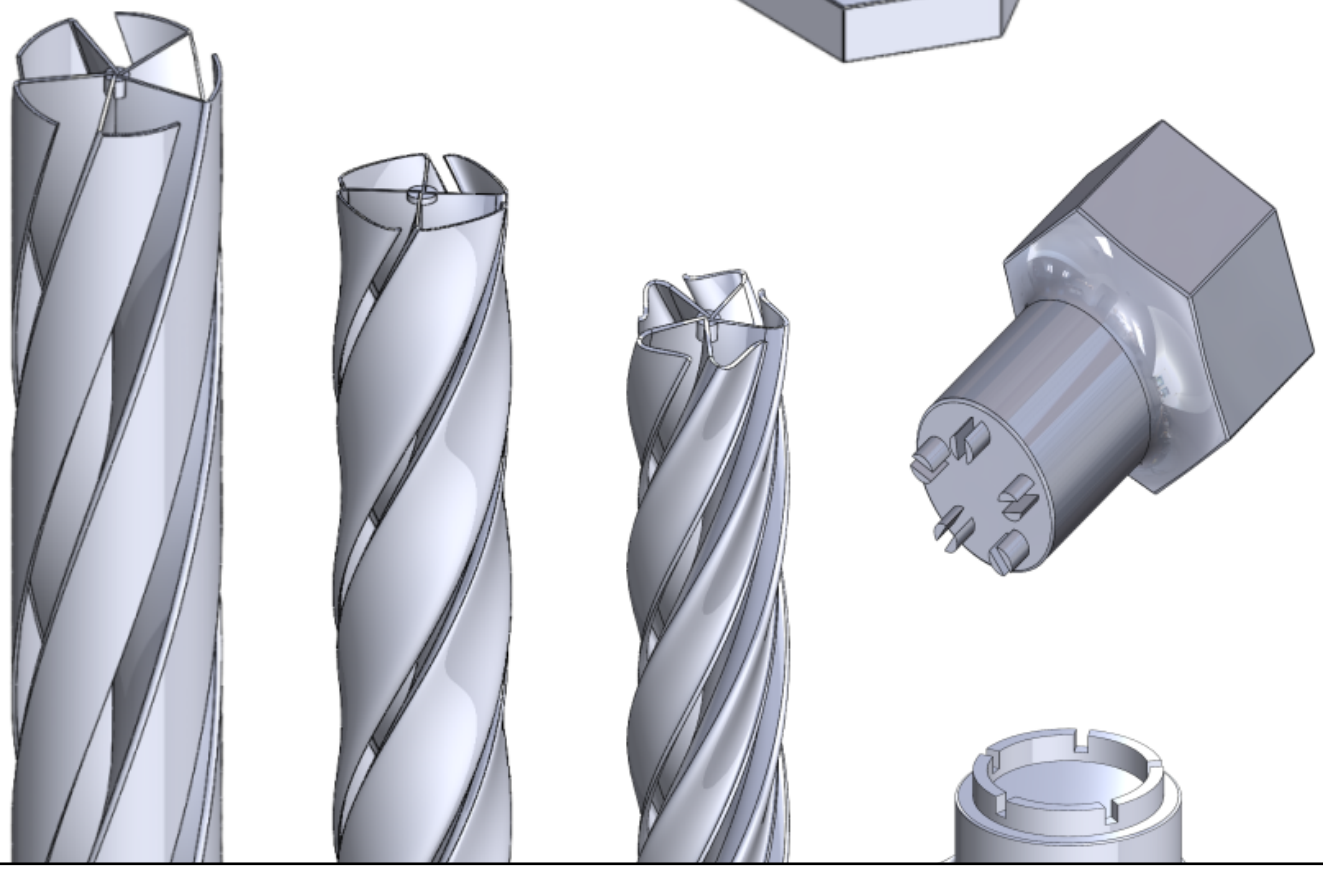

TU Delft Delft University of Technology

Challenge the future

0.9

THESIS TITLE:

SYNTHESIS OF NONLINEAR TORQUE-ANGLE PROFILE USING COMPLIANT HELICOIDAL SHELL JOINT

M.Sc. Thesis Report

For
ME-HTE MSc Thesis (ME56035)
at Delft University of Technology

by

SINA ABOUHEIDARI

M.Sc. Mechanical Engineering
(High-tech Engineering Track)

Supervisor: Dr. ir. Giuseppe Radaelli

Faculty of Mechanical Engineering

(Formerly known as 3mE)

The Department of Precision and Microsystems Engineering (PME)

Copyright © 2024 by S. ABOUHEIDARI
Delft University of Technology

Engineering is not only about making things work,
it's about making things work better for people.

Henry Petroski

CONTENTS

ABSTRACT

Compliant mechanisms, particularly helicoidal shell joints, present intriguing possibilities in mechanical design with applications in medical devices, robotics, automotive, and aerospace engineering. This research focuses on the synthesis of nonlinear torque-angle profiles using a compliant helicoidal shell mechanism such as gravity-balancing profiles. This study required a thorough exploration of the mechanism's diverse design variations through Finite Element Modeling (FEM) and more specifically, Isogeometric Analysis (IGA). Subsequently, a targeted optimization process is utilized, incorporating both global geometric parameter adjustments and localized modifications by using splines. The prominent challenge addressed is the synthesis of gravity balancing torque-angle profile, achieved by tailoring the output profile of a compliant shell mechanism through optimization. Considering the inherent sine function output of a pendulum during gravitational equilibrium, an algorithm is developed to optimize the mechanism's behavior to align with a sine function, hence enabling gravity balancing. Additionally, experimental validation was undertaken through manufacturing prototypes and conducting measurements to provide a crucial link between simulations and real-world behavior. The results of this research, encompassing optimized geometry and experimental data, are presented, and comprehensively discussed. This research contributes a numerical methodology that utilizes isogeometric analysis and optimization algorithm within the framework of finite element analysis for achieving nonlinear torque-angle profiles in complaint helicoidal shell mechanisms, such as gravity balancing profiles, offering valuable insights for possible applications in various engineering domains.

Keywords: Compliant mechanisms, complaint shell mechanisms, compliant joints, tunable joints, compliant revolute joints

1

INTRODUCTION

1.1. BACKGROUND

For centuries, mechanisms have made our lives simpler. Early examples include primary forms of wheels, gears, levers, and pulleys used by the Greeks and Romans [1]. Traditionally, mechanisms are composed of rigid parts that are joined together with pins, hinges, or other types of mechanical joints to enable the control and transfer of motion and force. However, the use of compliant materials in engineering has led to the development of compliant mechanisms that are flexible, lightweight [2], and may offer more simplicity in design [3]. Compliant mechanisms rely on the elastic deformation of their components to achieve the desired motion or force output. Early examples of using compliance to achieve certain functionalities include bow and arrow [4]. The benefits of compliant mechanisms can be classified into two main groups [4]:

- Cost savings, which include reductions in the number of parts, assembly time, and manufacturing complexity;
- Performance enhancements, such as improved precision, reliability, decreased wear, lower weight, and reduced maintenance.

The capacity of compliant mechanisms to store and release energy is another advantage. Flexible mechanisms can use the elastic deformation of their parts to store energy that can later be released to perform mechanical work [5]. They are thus desirable for where energy storage is essential, such as springs, beams, or other energy-storing elements.

Despite these advantages, the use of compliant mechanisms also presents some challenges. One of the primary challenges is the complexity of modeling and analysis [6]. Compliant mechanisms are highly nonlinear, and their behavior is difficult to predict without extensive testing and analysis. This can make the design process more challenging and time-consuming than the traditional, rigid-body mechanisms.

Compliant joints are a subset of compliant mechanisms employed in different applications as mechanical joints, offering various advantages such as increased precision, high reliability, compactness, energy efficiency, and a high level of freedom in design. These advantages make them suitable for various applications such as robotics, assistive medical devices, and aerospace applications. These mechanisms achieve their unique performance through the utilization of different designs, materials, structures, and working principles. This means to customize their performance for specific applications and profiles, several aspects of such mechanism can be modified and tailored for specific requirements. These variations lead to

a rather diverse set of compliant joints which differ in stiffness, range of motion, compliance, and mode of deformation. The ability of compliant joints to accommodate part misalignment is one of their main benefits. Traditional rigid joints need the mating parts to be precisely aligned, which can be challenging to do in practice. Conversely, because their parts deform elastically, compliant joints can accommodate minor misalignment [7]. Since there may be minor variations in the mating parts, they are ideal for applications where alignment is challenging.

Compliant joints vary significantly in their structure and functionalities, the degrees of freedom, the type of motion they transfer, and when it comes to compliance, the type of deformation that occurs in the joint. Translational joints, revolute joints, and universal joints are all different types of joints that could be made with compliant elements.

Howell et al. [5] have classified flexible elements as beams, revolute elements (including hinges, scissors, torsion, and Lamina Emergent elements), translational, universal compliant joints, and others. Additionally, compliant joints have also been classified as variations of either Notch-type joints or leaf springs [8]. In this classification, Notch-type joints achieve their compliance from an indentation or notch in the structure of the flexible element whereas deformation of an arrangement of leaf springs is the principle that the other compliant joints utilize to achieve their specific properties.

To assess the performance of compliant joints, different aspects can be prioritized and assessed. Trease et al. [8] have provided five criteria for the assessment of compliant joints. They are as follows:

- Range of Motion: In most cases, compliant revolute joints might offer a limited range of motion whereas rigid-body revolute joints usually offer an unlimited range of motion. The reason for this arises from the inherent properties of compliant mechanisms. In large deformations, the risk of reaching yield stress and entering the plastic deformation zone limits the range of motion as the plastic stress will lead to undesirable behavior of the joint by making it unreliable and inconsistent.

- Axis Drift: While for a precise motion, a fixed center of rotation is desirable, in compliant revolute joints, there is a possibility of drift in the axis of rotation which will lead to parasitic motion.

- Off-Axis Stiffness: An ideal compliant revolute joint will have high compliance in its respective axis of rotation while offering high stiffness (both rotational and translational) in other directions.

- Stress Concentration Effects: In any mechanical element, the issue of stress concentration, when a variation of geometry or material is present, is of concern to avoid the failure of the structure.

- Compactness: In some compliant joint mechanisms, the precision and functionality of the joint have a trade-off with its stiffness. While making the structure more compact is ideal where there is limited spacing in a mechanical design, it might cause the structure to have less off-axis stiffness [9].

1.2. RESEARCH PROBLEM

Synthesizing complaint joints can be approached with various objectives, methods, and structures. Literature includes examples of the synthesis of constant-torque mechanisms

[10, 11], as well as examples of nonlinear torque-angle profiles for specific applications such as the study by Hampali et. al. [9, 12] which is an example of compliant shells designed for a desirable output profile or achieving nonlinear torque-angle profiles using nonlinear springs [13]. These examples show the significance of designing complaint mechanisms for specific target profiles. In synthesizing nonlinear torque-angle profiles for compliant joints, one significant objective is gravity-balancing profiles, examples of which include [14, 15].

To synthesize nonlinear torque-angle profiles, one approach is to analyze bistable structures and optimize their geometry to manipulate their output. The helicoidal shell mechanism studied by Radaelli [16] is an example of constant-moment compliant joint. This joint exhibits a gradual increase in the deformed region as the structure is twisted, this means the applied torque is only affected by the portion of the structure that is deformed, and not the structure as a whole. While this behavior can be utilized to obtain neutrally stable linkage mechanisms [16], one promising potential is the possibility of utilizing this behavior in the optimization of this geometry to achieve alternative nonlinear profiles. However, to achieve possible negative stiffness regions, variations of this structure need to be studied such as the introduction of a flange to this structure and the possibility of observing bistable behavior such as the one seen in the study by Nobaveh et. al. [17].

While studying and analyzing the different nonlinear behaviors shown by a compliant joint is of importance, it is also important to analyze the tunability of these structures, and a key objective for this matter is the possibility of introducing a gravity-balancing profile which will be the focus of this study.

1.3. RESEARCH OBJECTIVE

The key research objective of this study is to develop a design based on a helicoidal shell mechanism to synthesize a nonlinear torque-angle profile. Furthermore, this design is utilized by geometric optimization to achieve a gravity-balancing torque-angle profile. Additionally, the objective is to complement this study by developing prototypes and conducting experimental measurements to link computational simulation to real-world behavior.

1.4. RESEARCH FRAMEWORK

This research is conducted by a comprehensive study of several design variations of the helicoidal shell mechanism, originally studied by Radelli [16], and selecting possible design variations to be further studied and optimized for gravity-balancing profiles. This study is done by computational simulation through Finite Element Modeling (FEM), and more specifically, Isogeometric Analysis (IGA). In addition to that, prototypes with Stereolithography 3D printing are developed and manufactured for experimental measurements.

1.5. THESIS ORGANIZATION

The second chapter of this thesis is a research paper dedicated to the main objective of this study. The third chapter is the conclusion of this study and suggestions for further avenues of research to enhance the work presented here and provide further insight into this field. The first appendix is dedicated to a short theoretical background for the numerical approach utilized in this study. The second appendix will provide an overview of alternative designs, and the third appendix will provide supplementary optimization results that are not included in the main paper but might interest readers for deeper insights. The last appendix will cover

another target profile that is achieved with the methodology of this research and shows the potential of the studied structure to be tuned for engineering applications.

REFERENCES

[1] *The birth of engineering: history of mechanisms that set the world in motion - Max Polyakov*. Sept. 2022. URL: https://maxpolyakov.com/the-birth-of-engineering-the-mechanisms-that-set-the-world-in-motion/.

[2] H. W. Hufenbach, H. K.-h. Modler, O. Täger, D.-I. N. Modler, and D.-I. O. Renner. "CONTRIBUTION TO THE DEVELOPMENT OF ACTIVE COMPLIANT LIGHTWEIGHT MECHANISM STRUCTURES". In: *IFAC Proceedings Volumes* 39.16 (Jan. 2006), pp. 1082–1085. DOI: 10.3182/20060912-3-de-2911.00186. URL: https://doi.org/10.3182/20060912-3-de-2911.00186.

[3] S. P. Jagtap, B. B. Deshmukh, and S. Pardeshi. "Applications of compliant mechanism in today's world – A review". In: *Journal of physics* 1969.1 (July 2021), p. 012013. DOI: 10.1088/1742-6596/1969/1/012013. URL: https://doi.org/10.1088/1742-6596/1969/1/012013.

[4] L. L. Howell. *Compliant mechanisms*. John Wiley & Sons, Aug. 2001.

[5] L. L. Howell, S. P. Magleby, and B. C. Olsen. *Handbook of Compliant Mechanisms*. Wiley, Feb. 2013. DOI: 10.1002/9781118516485.

[6] H. Li and G. Hao. "Constraint-force-based approach of modelling compliant mechanisms: Principle and application". In: *Precision Engineering-journal of The International Societies for Precision Engineering and Nanotechnology* 47 (Jan. 2017), pp. 158–181. DOI: 10.1016/j.precisioneng.2016.08.001. URL: https://doi.org/10.1016/j.precisioneng.2016.08.001.

[7] M. A. C. G, Lvez-Zúñiga, A. Aceves-L, and Pez. "A Review on Compliant Joint Mechanisms for Lower Limb Exoskeletons". In: *Journal of Robotics* (Aug. 2016). DOI: 10.1155/2016/5751391. URL: https://doi.org/10.1155/2016/5751391.

[8] B. P. Trease, Y.-M. Moon, and S. Kota. "Design of Large-Displacement Compliant Joints". In: *ASME Digital Collection* (Nov. 2004). DOI: 10.1115/1.1900149. URL: https://doi.org/10.1115/1.1900149.

[9] S. Hampali, A. P. S, and G. K. Ananthasuresh. "A Tunable Variable-Torque Compliant Hinge Using Open-Section Shells". In: *Journal of Mechanisms and Robotics* 12.6 (Dec. 2020). DOI: 10.1115/1.4047440.

[10] H. N. Prakashah and H. Zhou. "Synthesis of Constant Torque Compliant Mechanisms". In: *Journal of Mechanisms and Robotics* 8.6 (Aug. 2015). DOI: 10.1115/1.4034885.

[11] C.-W. Hou and C.-C. Lan. "Functional joint mechanisms with constant-torque outputs". In: *Mechanism and Machine Theory* 62 (Apr. 2013), pp. 166–181. DOI: 10.1016/j.mechmachtheory.2012.12.002. URL: https://doi.org/10.1016/j.mechmachtheory.2012.12.002.

[12] S. Hampali, P. Anoosha, and G. K. Ananthasuresh. *An Open-Section Shell Designed for Customized Bending and Twisting to Ease Sitting and Rising in a Chair*. Springer Nature, Jan. 2019. DOI: 10.1007/978-981-10-8597-0\{_}36.

[13] A. Ahmed and H. Zhou. "Spring synthesis for nonlinear Force-Displacement function". In: *International journal of engineering research and technology* 3.3 (Mar. 2014). URL: https://www.ijert.org/research/spring-synthesis-for-nonlinear-force-displacement-function-IJERTV3IS030376.pdf.

[14] G. Radaelli and J. L. Herder. "Gravity balanced compliant shell mechanisms". In: *International Journal of Solids and Structures* 118-119 (July 2017), pp. 78–88. DOI: 10.1016/j.ijsolstr.2017.04.021. URL: https://doi.org/10.1016/j.ijsolstr.2017.04.021.

[15] G. Radaelli and J. L. Herder. "A monolithic compliant large-range gravity balancer". In: *Mechanism and Machine Theory* 102 (Aug. 2016), pp. 55–67. DOI: 10.1016/j.mechmachtheory.2016.03.015. URL: https://doi.org/10.1016/j.mechmachtheory.2016.03.015.

[16] G. Radaelli. "Reverse-twisting of helicoidal shells to obtain neutrally stable linkage mechanisms". In: *International Journal of Mechanical Sciences* 202-203 (July 2021), p. 106532. DOI: 10.1016/j.ijmecsci.2021.106532. URL: https://doi.org/10.1016/j.ijmecsci.2021.106532.

[17] A. A. Nobaveh, J. L. Herder, and G. Radaelli. "A compliant Continuously Variable Transmission (CVT)". In: *Mechanism and Machine Theory* 184 (June 2023), p. 105281. DOI: 10.1016/j.mechmachtheory.2023.105281. URL: https://doi.org/10.1016/j.mechmachtheory.2023.105281.

2

MAIN PAPER

Synthesizing gravity-balancing torque-angle profile using helicoidal shell joints

Abstract: Compliant mechanisms, particularly helicoidal shell joints, present intriguing possibilities in mechanical design. This paper focuses on the optimization and synthesis of a gravity-balancing torque-angle profile using a compliant helicoidal shell mechanism. The investigation commences with a meticulous exploration of the mechanism's diverse design variations through Finite Element Modelling (FEM) and more specifically, Isogeometric Analysis (IGA). Subsequently, a targeted optimization process unfolds, incorporating both global geometric parameter adjustments and localized modifications using splines. The prominent challenge addressed is the gravity balancing profile of the compliant mechanism, achieved by tailoring the torque-angle output profile. Considering the inherent sine function output of a pendulum during gravitational equilibrium, an algorithm is developed to optimize the mechanism's behavior to align with a sine function, hence enabling gravity balancing. Experimental validation provides a crucial link between simulations and real-world behavior. Results, encompassing optimized geometry and experimental measurements, are presented and comprehensively discussed. This paper contributes a numerical methodology for achieving gravity balancing in compliant helicoidal shell mechanisms, offering valuable insights for applications in various engineering domains.

2.1. INTRODUCTION

Compliant mechanisms, with their ability to exploit material flexibility for functional motion, have become a focal point of research in mechanical engineering. Compliant shells, exhibit intriguing characteristics that make them suitable for various applications [1–4]. These characteristics include the lack of friction, play, wear, and the requirement for assembly, or lubrication [5] as well as high tunability, spatial, and slender design [2]. One notable example of such mechanisms is a compliant revolute joint based on reverse twisting of helicoidal shells that has been proposed and studied thoroughly by Radaelli [5]. This mechanism offers low axis drift, high support stiffness, and a large range of motion. It exhibits a gradual increase of deformation in the reversed region as the joint is twisted, resulting in a constant reaction moment. While this structure depicts an intriguing behavior that can be utilized to achieve a range of neutrally stable linkages, the possibility of alternative nonlinear torque-angle profiles remains an interesting aspect, yet to be discovered and to answer this question, the effect of design parameters and the shape of this structure on its torque-angle profile, need to be thoroughly studied. Literature includes applications of compliant mechanisms for constant torque profiles [2, 6, 7] as well as nonlinear torque profiles [8], including examples of profiles with negative-stiffness region [9], and bistability [10, 11].

Gravity balancing is a critical objective in various mechanical systems [12–16], and can be pursued through the tailoring of the torque-angle output profile through a recreation of the sine function profile, which is observed in dynamics of a pendulum, during gravitational equilibrium. Therefore, a sine function to govern the torque-angle relationship can be introduced as the objective for this purpose. By employing the knowledge of the alternative behaviors exhibited by different variations of this helicoidal shell, through geometry optimization, a gravity-balancing torque-angle profile can be introduced. This study addresses this challenge, combining isogeometric analysis within the framework of finite element modeling, and geometric optimization to synthesize a gravity-balancing torque-angle profile for a helicoidal shell mechanism. In the literature, there are examples of compliant gravity-balancing structures [17–20], and non-compliant structures [21–24]. While in many examples in the literature, conventional springs are utilized for the synthesis of a desired output profile, [8, 25–27], this study utilizes compliant joints to achieve this objective.

This research contributes a comprehensive analysis of variations in compliant helicoidal shell mechanism and, more critically, introduces a methodology for achieving gravity-balancing behavior through a combination of isogeometric analysis and optimization techniques. The aim is to demonstrate the effectiveness of this approach in tailoring the torque-angle profile to emulate a sine function, thereby ensuring a gravity-balancing behavior in the helicoidal shell mechanism. This study leads to the identification of a specific variation of the helicoidal shell mechanism, namely, an L-shape design, which is first analyzed parametrically, and then to achieve a gravity-balancing profile, optimization is carried out by employing both global and local geometric parameter approaches. The former enables an effective adjustment of the mechanism's global geometry, while the latter, utilizes the inherent implementation of splines in isogeometric analysis to facilitate more fine-tuned modifications in the shape of this structure.

Section 2.2 delves into the methodology, elucidating the finite element modeling process and detailing both the global and local geometric parameter optimization approaches. Experimental validation procedures are outlined in Section 2.2.3. Section 2.3 unfolds the outcomes of this re-

search, presenting optimized geometry (Section 2.3.1 and 2.3.2) and experimental measurements (Section 2.3.3). In Section 2.4, these results are thoroughly discussed, providing insights into the effectiveness of the proposed gravity balancing methodology. Finally, Section 2.5 concludes this study, summarizing key findings, addressing limitations, and suggesting avenues for future research.

2.2. METHODOLOGY

Discovering the potential nonlinear profiles exhibited by the helicoidal shell mechanism and synthesis of a nonlinear torque-angle profile requires analyzing different methods to introduce alternative behaviors to the helicoidal shell joint. The compliant shell mechanism studied by Radaelli [5] exhibits a constant moment profile. The underlying cause of this behavior is the fact that as the angle of twist increases, the portion of the shell that reverses its direction of twist also increases. This structure which consists of at least three shells with a common edge, follows the assumption of inextensible shells which results in the preservation of the Gaussian curvature as the structure is twisted. An intriguing behviour occurs when the twisting is introduced gradually. When a relative rotation is applied to the two ends of the joint, a section of the helicoid rapidly transitions into a reverse-twist state due to the low deformation energy associated with that mode. Meanwhile, the remaining portion of the helicoid remains nearly unaffected. This deformation state gives rise to two distinctive and peculiar phenomena. The initial observation is that the length of the reverse-twist region is directly proportional to the applied rotation angle. Consequently, the elastic energy shows a linear increase with the applied rotation angle. According to the definition of generalized conservative forces, the reaction moment corresponding to the applied rotation remains constant, resulting in zero rotational stiffness. This condition of a constant moment and zero stiffness persists until the entire joint is reversed. The second notable phenomenon is that when the rotation angle is kept constant, the reverse-twist region's position can be adjusted along the structure without altering its length. This implies a constant total stored energy, and each position of the reverse-twist region achieves static equilibrium, rendering it neutrally stable. Additionally, the reversed-twist region can be vertically adjusted by rotating it around the middle axis, essentially creating a zero-moment rotational joint [5].

Figure 2.1 shows the schematic of this compliant helicoidal shell mechanism and its geometrical parameters. Radaelli [5] has studied the effect of the geometric parameters, the thickness(t), width(w), and angle of twist(α) (the pitch), analytically and numerically as shown in Figure 2.2 and from these graphs the effect of geometric parameters can be observed to have a prominent shifting effect on the torque-angle profile when they are changed as a single varying parameter. The analytical results have been also compared with the experimental data in this study [5]. The reference geometry has a thickness of $0.4 \times 10^{-3}\, m$, width of $0.1 \times 10^{-1}\, m$, angle of twist equal to $\frac{\pi}{0.1}\, rad\, m^{-1}$.

The study of this helicoidal shell by Radaelli [5] lays the foundation for the research presented here. To acquire an overview of alternative torque-angle profiles of this helicoidal shell, several design variations based on the helicoidal shell studied by Radaelli [5] were developed and studied, and the results were used for optimizing the torque-angle profile for gravity balancing function. The next sections will show how these design variations were developed, studied, and later optimized for gravity balancing.

2.2.1. FINITE ELEMENT ANALYSIS

The primary tool employed in this research is Isogeometric Analysis (IGA) within the

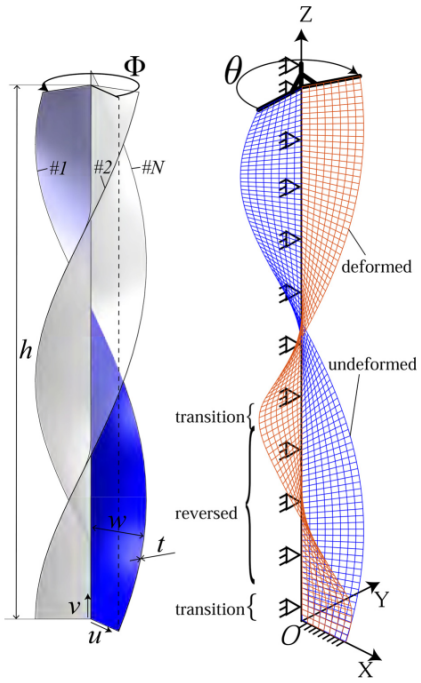

Figure 2.1.: a) Schematic of helicoidal shell and its geometric parameters and b) The FEM model for helicoidal shell [5].

framework of Finite Element Modeling (FEM), a schematic of the finite element model is seen in Figure 2.1. The isogeometric study is based on a program implemented in MATLAB software based on the work of A.P. Nagy [28]. For this study, the geometry is defined by a network of control points, each having three coordinates in the cylindrical coordinate system, radius, height, and angle. These coordinates are later transformed into a Cartesian coordinate system. The network of control points is then utilized by a Non-uniform rational B-spline (NURBS) algorithm to create a surface for the study domain. In the base helicoidal shell mechanism, the middle edge nodes are constrained, and the bottom edge nodes are clamped to be fixed while the upper edge nodes are clamped to be rotated with a desired angle. In some variations, such as the study of an L-shape cross-section, the web is clamped similarly, whereas the flange is free to allow for warping. The underlying mathematical model for the simulation of this problem is the Kirchhoff-Love theory of plates.

Several variations of the base helicoidal shell (the original mechanism studied by Radaelli [5]) were analyzed for this research. One key aspect of this helicoidal shell mechanism is critical in developing alternative designs, which is the gradual deformation of the shell in the direction of its height when twisted. This means if the same behavior were to be recreated in modified designs, as the structure is twisted, only the change of geometry in the deformed region is observed in the torque-angle profile, meaning the possibility of local control for the behavior of this joint. The selected design variation which is comprehensively studied in this research and optimized for gravity-balancing behavior, is the helicoidal shell with an L-shape cross-section. To create this cross-section, a curved flange is designed based on the cylindrical coordinates, therefore, the flange is shaped as a circular arc. To control the shape of this flange, two geometrical factors were created, a length factor (L_f) and a sharpness factor (S_f). The length factor is the ratio of the flange length (arc length) to the width of the shell (web length), and the sharpness factor is defined as the ratio between the radius of the endpoint of the arc at θ_{arc} (where θ_{arc} is the arc angle) and the width of the shell (web length). In theory, the minimum value for the length factor can be as low as zero which is the simple helicoidal shell that does not have an additional flange, and the minimum value for the sharpness factor is one, as the minimum radius of any point on the arc is the same as the shell width. The control points on the flange starting from the endpoint of the web to the endpoint of the arc at θ_{arc}, are defined linearly varying from w to $S_f \times w$. A higher value for the sharpness factor translates to a less sharp L-shape. Figure 2.3 shows the schematic of the cross-section of the L-shape design. In this schematic, w is the width of the web, r is the radius

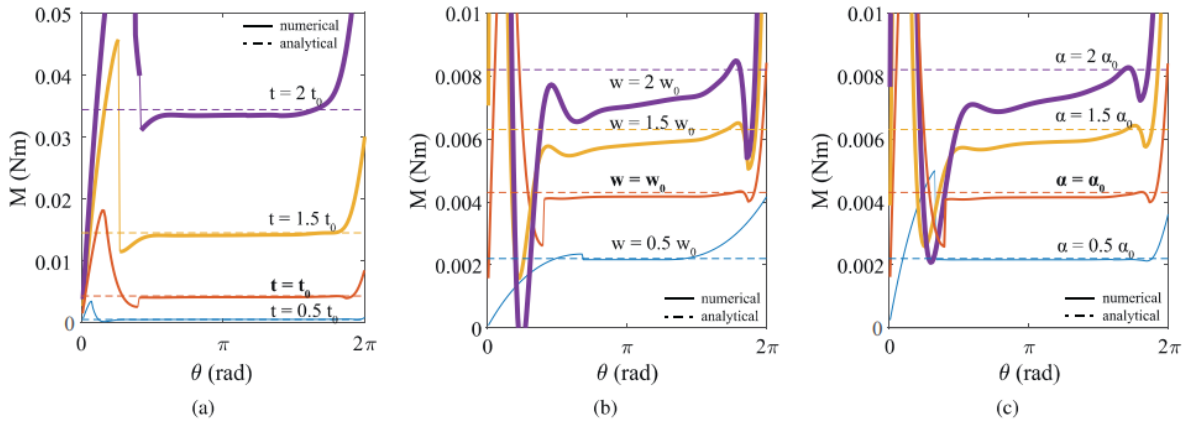

Figure 2.2.: Torque-angle profile for varying a) thickness b) width, and c) angle of twist [5].

of the endpoint of the flange, s is the arc corresponding to the flange, and r' represents an alternative radius of flange if S_f exceeds one. The length factor and the sharpness factor can be defined as follows:

$$L_f = \frac{s}{w} \tag{2.1}$$

$$S_f = \frac{r'}{w} \tag{2.2}$$

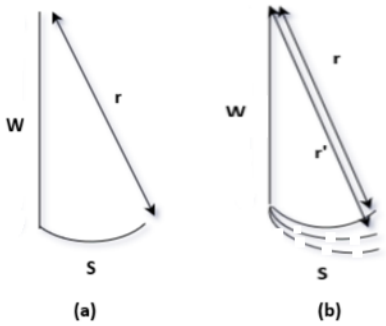

Figure 2.3.: a) Schematic of L-shape design and b) Variation of sharpness factor

The finite element model is the simulation of a single-shell structure. However, the helicoidal shell joint can have a desired number of shells with a minimum number of 3 [5]. The output profile of this joint corresponds to the summation of the resisting moments of these shells. Figure 2.4 shows the cross-section of an L-shape helicoidal shell joint with 6 shells. The material properties used for simulation correspond to Nylon (PA12) are presented in Table 2.1 [5].

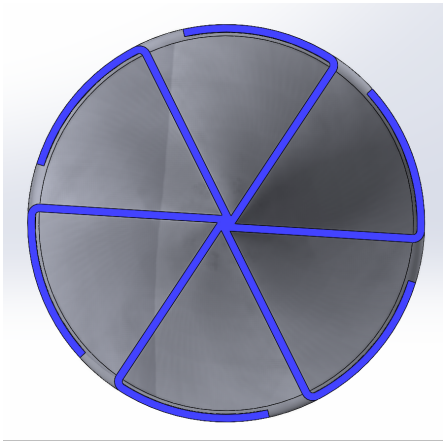

Figure 2.4.: Cross-section view of the L-shape helicoidal shell joint

Table 2.1.: Material Properties for FEM

Property	Value	Unit
Young's Modulus	1.8	Gpa
Poisson's Ratio	0.38	-

2.2.2. OPTIMIZATION IMPLEMENTATION

The optimization algorithm is first implemented for the base helicoidal shell design studied by Radaelli [5], and then it

is utilized for the L-shape helicoidal shell. The choice of L-shape design is due to its ability to exhibit a bistable behavior and a negative stiffness region. Having these characteristics leads to a potential for profiles similar to a sine function, and hence, the possibility of introducing gravity-balancing profiles for this compliant shell mechanism.

To achieve a gravity-balancing profile through geometric design optimization, two different approaches are employed, Global Geometric Parameters Approach, and Local Geometric Parameters Approach which are discussed in the following sections. For this study, each optimization approach was simulated four times, with four different angle windows, 90, 180, 270, and 360 degrees. To achieve a gravity-balancing profile, the sine function is used as a target function for optimization. The reason for this is that a simple pendulum with mass m, connected at the end of a rod of negligible mass with the length L, requires a counteracting torque equivalent to $mgLsin(\theta)$. To shape the output profile of the helicoidal joint, the simulated torque response is normalized and compared to a sine function with an amplitude of one. The comparison is implemented by a root-mean-square-error calculation, which is minimized as the objective function by the optimizer to achieve the target behavior. This is shown in Equation 2.3. $\tilde{T}_{target}$ is the target normalized torque values corresponding to a sine, $\tilde{T}$ is the normalized simulated torque, and n is the number of data points.

$$RMSE = \sqrt{\frac{(\tilde{T}_{\text{target}} - \tilde{T})^2}{n}} \tag{2.3}$$

GLOBAL GEOMETRIC PARAMETERS APPROACH

The first optimization approach is optimizing global geometric parameters, which refers to parameters that change the structure as a whole, and the cross-section remains constant throughout the height of the helicoidal shell. While the effect of the main geometrical parameters of the base helicoidal shell joint has been studied by Radaelli [5], the proportionality of these factors affects the behavior of the joint and is, therefore, the reason to include them as optimization variables.

- Thickness (T)
- Width (W)
- Pitch (P)
- Height (H)
- Length Factor (L_f)
- Sharpness Factor (S_f)

The optimization of the L-shape design for obtaining a gravity-balancing profile with this approach is done by gradually increasing the complexity of the optimization, starting with only the length factor and sharpness factor for the L-shape design, and then implementing a six-variable optimization including the four fundamental geometric parameters, T, W, P, H, in addition to the length factor and the sharpness factor which are the additional geometric parameters for the L-shape design variation. Table 2.2 includes the optimization parameters their set value, and the lower and upper bounds used in the optimization.

LOCAL GEOMETRIC PARAMETERS APPROACH

This approach is pursued based on the inherent characteristic of the helicoidal shell mechanism studied by Radaelli [5], where deformation happens locally and is gradually increased along the height of the shell when the structure is twisted. This proposed the idea for local control over the geometry introducing an evenly spaced out set of control points along the height and optimizing the geometry by controlling the four parameters each set of the control points possesses. This results in a cross-section and geometry that varies along the height

Table 2.2.: Optimization parameters and their bounds

Parameter	Value	Lower Bound	Upper Bound
T (Thickness)	0.0004[m]	0.0001	0.001
W (Width)	0.01[m]	0.001	0.02
P (Pitch)	0.2[m]	0.1	0.3
H (Height)	0.1[m]	0.01	0.2
L_f (Length Factor)	0.75	0.1	2
S_f (Sharpness Factor)	1	1	2.5

of the helicoidal shell. The local geometric parameters introduced for each set of evenly spaced out control points are

- Radius (Width)
- Angle (Pitch)
- Length Factor (L_f)
- Sharpness Factor (S_f)

As the number of control points along the height of the shell in this approach is decreased compared to the defined geometry that was discussed in 2.2.1, spline refinement is required to interpolate other points in between these control points to create a surface. First, a set of five and then a set of ten evenly spaced control points are introduced along the height of the helicoidal shell, which means the height remains constant. Naturally, increasing the number of control points makes the optimization more complex in computation while it may increase the refinement of the results. Additionally, it should be noted that thickness acts as a global parameter here and remains constant.

2.2.3. EXPERIMENTAL VALIDATION

While the finite element software and the corresponding model have been validated in the previous study [5], to compare the simulated behavior of the L-shape helicoidal shell joint with the real behavior of a prototype, two CAD models were created with five symmetrical shells as seen in Figure 2.5 which were later printed with Stereolithography (SLA) 3D printing method using Tough 1500 resin [29] with Form 3+ 3D printer [30]. A tensile machine was used for the experiment, twisting the structure with a constant rate of $\frac{2\pi}{60} rad/s$. Two experiments were conducted; one for the L-shape design with the set default geometric values, as seen in Table 2.2, and one to validate the results of a gravity-balancing optimized profile for target 90 degrees sine function. Figure 2.5 (a) shows the prototype corresponding to the former which has attached clamps and (b) corresponds to the latter with separate detachable clamps. The CAD model for the default L-shape design includes two hexagon-shaped ends to aid clamping in the tensile machine. The hexagon-shaped clamps are attached to a cylindrical part which is fixed to the upper and lower edges of the helicoidal shell. This design allows space for the warping of the shells in their flange. However, the prototype for a 90-degree optimized gravity-balancing profile has separate clamps to minimize the stress concentration on the lower edge of shells by minimizing the contact surface at gripping points and avoiding structure failure. Both prototypes were printed with the SLA method and Tough 1500 resin. The simulation results for comparison are also simulated and optimized respectively for material properties of Tough 1500. A Young's modulus of $E = 1.5GPa$ and a Poisson's ratio of $\nu = 0.35$ was used for the simulation. The experiment of the default L-shape design was done in differ-

ent stages with each having an increased range of twist with angles of 90, 180,270, and 340 degrees. Figure 2.6 shows the picture of the 3D-printed prototype and the test setup for the experimental measurement.

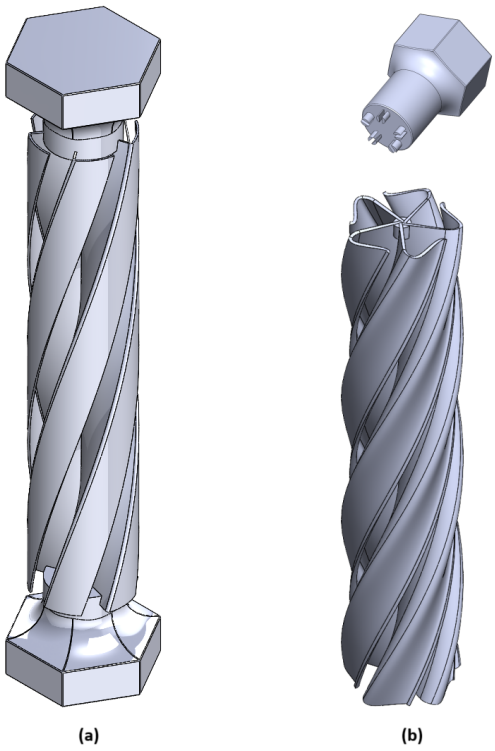

Figure 2.5.: Schematic of the CAD models created for the experiment: (a) Default L-shape design (b) Optimized L-shape design for 90-degree gravity-balancing profile

2.3. RESULTS

In section 2.2, the geometric analysis of the base helicoidal shell was mentioned. It should be noted that due to the working principle of this particular structure as discussed previously, the effect of height was not studied as the structure exhibits a gradual deformation along the height. In other words, for a constant angle of twist, the deformed region is dependent on the pitch, and for a constant pitch, height allows for a certain maximum twisting angle. This, however, is not true for the L-shape design, as the bistable behavior shows the deformation of the structure as a whole as well as gradual deformation along the height. In this sense, the L-shape shell acts as a hybrid between the total deformation of cross-sections along the height, and complete gradual deformation seen in the base helicoidal shell mechanism. In the next section, the impact of geometric factors on the L-shape design variation of the compliant helicoidal shell mechanism is presented, and subsequently, the result of the optimization will be presented, for both the global geometric and local geometric parameters approach. For the optimization results, the normalized resisting moment is used for shaping and comparison of the torque-angle profile. Optimization is done and presented by a step-by-step increase of the target angle window. It should be noted that not all structures simulated based on optimized solutions allow for a full twist in the target optimized range, meaning they result in structure failure when

Figure 2.6.: 3D-printed prototype and the test setup

they are twisted for the full targeted angle window.

Figure 2.7 shows the effect of the six geometric variables on the torque-angle profile of the L-shape design. While the effect of multiple factors acting simultaneously on the torque-angle output of the structure can be difficult to decompose in optimization results, the effect of a single variable provides valuable insights into the impact of each geometric design variable.

As seen in Figure 2.7, increasing the thickness, which leads to a bulkier structure as a whole, creates an overall higher stiffness in the structure, causing a shift in the resulting torque-angle profile and higher resistance to being twisted. The resisting moment exhibits an approximate twofold increase for every one-fold increase in thickness.

As for the width, the effect is somehow similar to thickness, but less significant, and affects the peaks and valleys more prominently. However, the constant torque region between the peak and valley does not change significantly, due to their small magnitude, as well as the location of the peak and the valley.

As for the pitch and the height, their effect is in a sense similar to each other and leads to the scaling of the torque-angle profile along the angle range. This means how much of the shell's behavior is observed if the twisting angle is the same, as well as other geometric variables. However, the effect of height on scaling the torque-angle output is more prominent, with the effect of increasing the height being similar to decreasing the pitch and vice versa.

As for the length factor, it affects the constant torque region of the profile, as well as the location of the peaks. As the length factor increases, the constant region gets steeper but continuing this increase and having a higher length factor from a certain point, flattens the constant region again and this increase fully changes and deviates the behavior of the structure, and a bistable structure can no longer be seen. As seen in the simulations, it was observed that the length factor drastically affects the hybrid behavior of the L-shaped helicoidal shell. While the original helicoidal shell shows gradual deformation, L-shape variation shows a gradual deformation as well as deformation of the structure as a whole, therefore a hybrid between these two extremes is seen. Decreasing the length factor shifts the behavior to more gradual deformation and vice versa.

The effect of the sharpness factor is very significant as it also changes the hybrid dynamic of this structure, higher sharpness factors result in structures that behave more similarly to the original helicoidal shell, therefore a more flat constant region is seen, while lower sharpness factor, pushes the behavior more towards a sine shape, decreasing the slope of the bistable region.

2.3.1. OPTIMIZED GEOMETRY FROM GLOBAL OPTIMIZATION APPROACH

The main difference between the base helicoidal shell and the L-shape variation is the introduction of a flange and the changed cross-section. The length factor (L_f) and the sharpness factor (S_f) are the two primary factors affecting this cross-section. Figure 2.8 shows the optimized profile for 90, 180, 270, and 360-degree windows by optimizing the length factor and the sharpness factor. While the balanced profile for the 90-degree target window shows a line closer to a straight line, for larger angle windows the balanced profile is very much deviated from a straight line.

While the length factor and the sharpness factor provide a significant level of control on the behavior of this compliant joint, without utilizing all six variables emulating a sine function is not achieved. Therefore an optimization with all six variables is presented in Figure 2.9 for 90 and 180

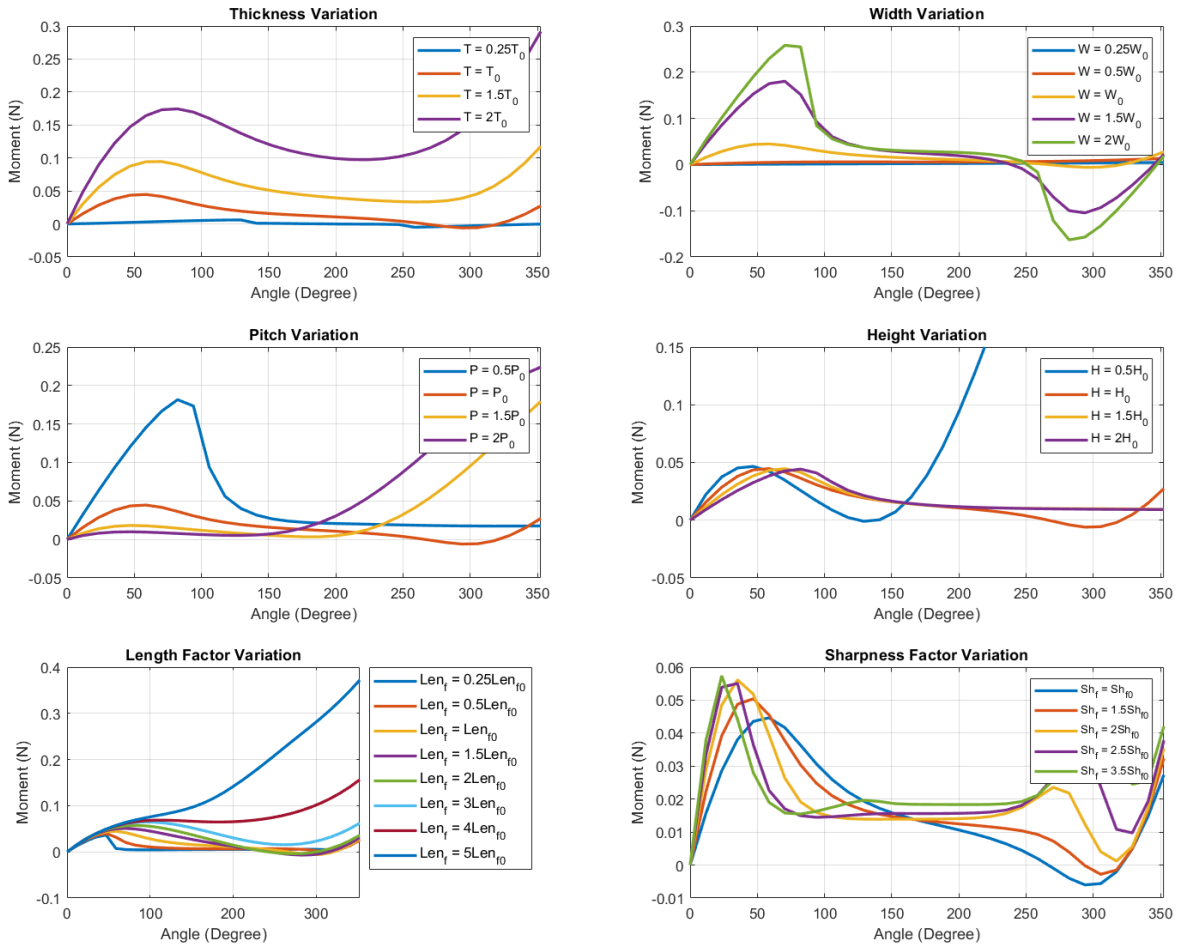

Figure 2.7.: L-shape Design: effect of geometric parameters

degrees. While for the 90-degree angle window, the balanced profile is close to a straight line (gravity-balanced) optimization for angles above 180 does not yield a sine function. This can also be seen in Figure 2.9 (b) in angles close to 180 degrees as the balanced profile deviated from a straight line.

2.3.2. OPTIMIZED GEOMETRY FROM LOCAL OPTIMIZATION APPROACH

The global geometric approach allows for the optimization of geometric variables that affect the whole structure; however, by utilizing spline refinements, optimization can be applied on a local scale, hence the possibility of allowing for a higher level of control of the torque-angle profile and fine-tuning the output of the joint. This approach starts with the base helicoidal shell joint, and it is then applied to the L-shape design variation.

Figure 2.10 shows the optimization result for the base helicoidal shell by using five control points in the target window of 90 and 180 degrees by local variation of radius (width) along the height (in total five optimization variables). While this shows a close profile to gravity-balancing for the range of 90 degrees, larger target windows are not possible as this structure does not exhibit a bistable behavior.

If the number of control points is increased, and ten points are used for optimization of both the radius (width) and angle (in total twenty optimization variables), a nearly

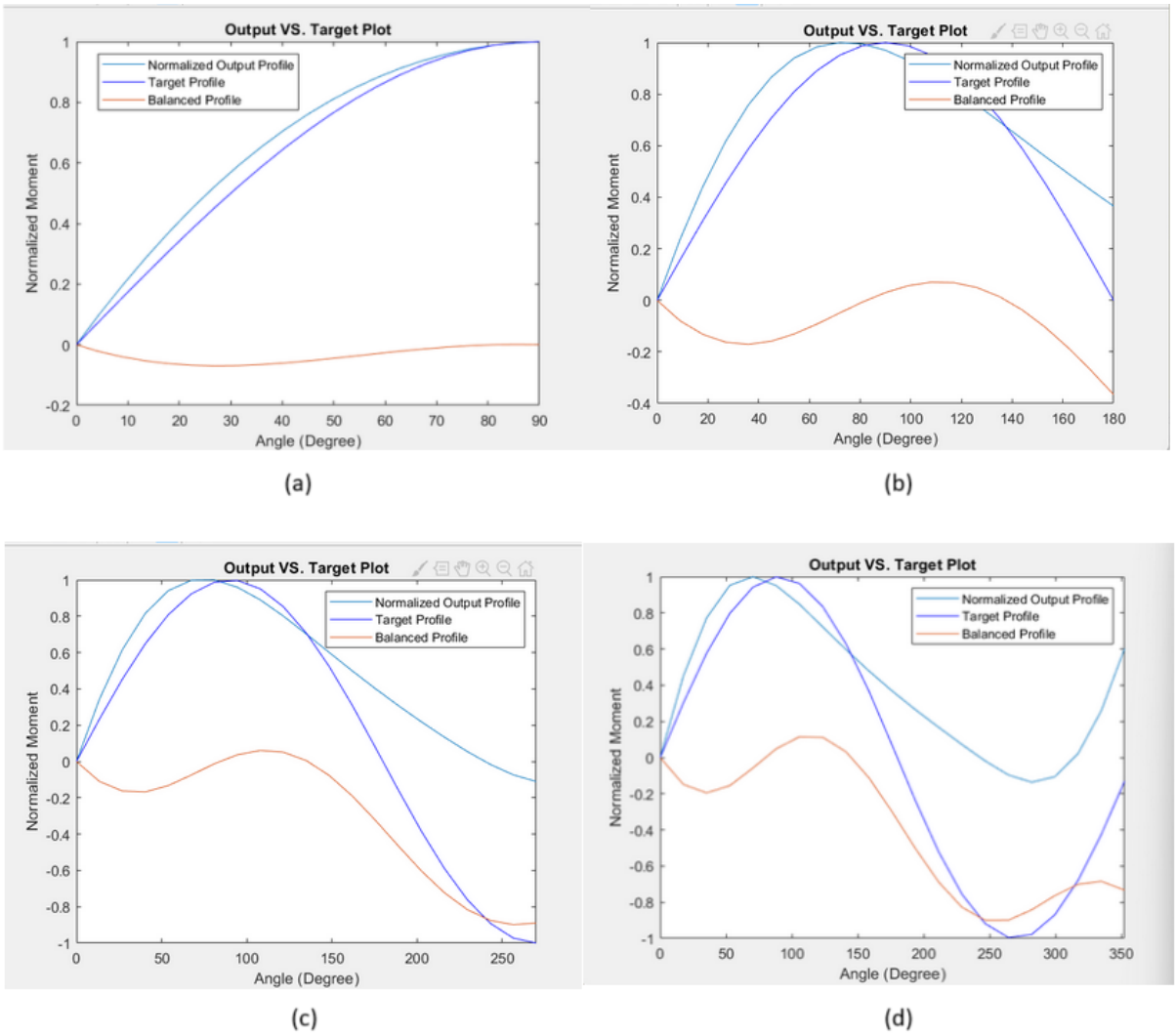

Figure 2.8.: The optimized torque-angle profile, based on the variation of L_f and S_f for a) 90, b) 180, c) 270 d) 360 degrees.

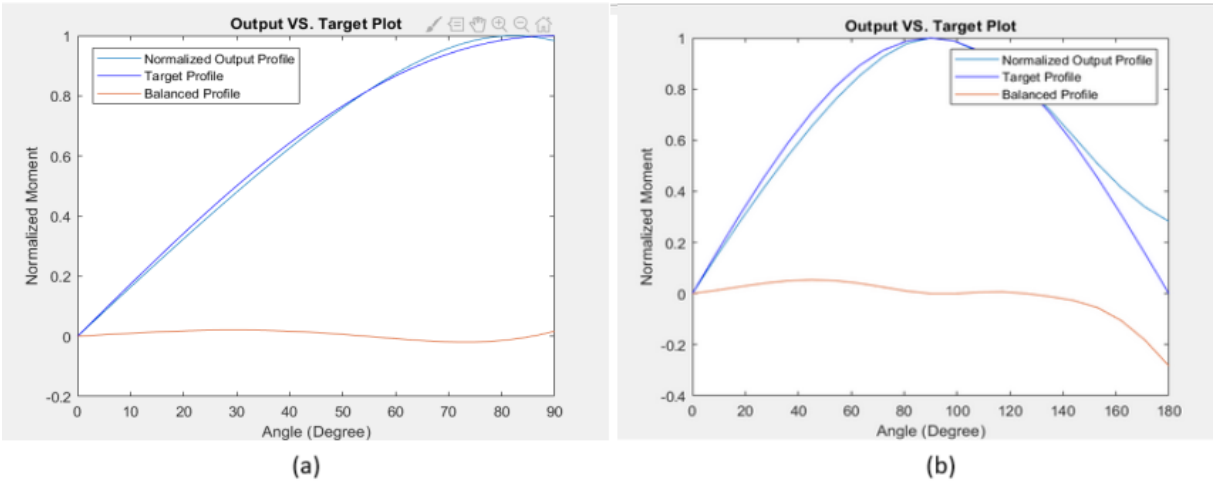

Figure 2.9.: The optimized torque-angle profile, based on the variation of all six geometric variables for a) 90, b) 180 degrees.

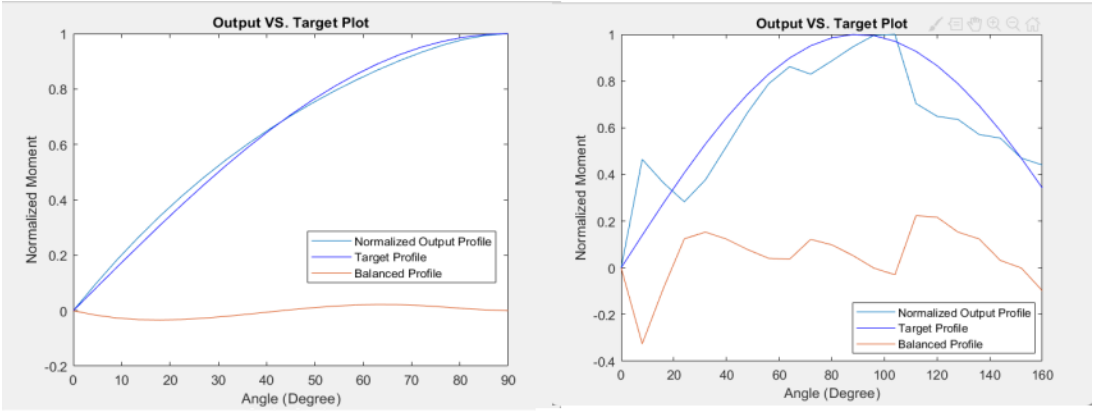

Figure 2.10.: The optimized torque-angle profile for the base helicoidal shell, based on the variation radius (width) along the height for a) 90, b) 180 degrees.

perfect balanced torque-angle profile can be produced with the base helicoidal shell joint as seen in Figure 2.11.

The local optimization approach for the L-shape variation introduces the possibility of a more complex optimization by adding two new variables; the length factor and the sharpness factor. Figure 2.12 shows the optimized profile of the L-shape helicoidal shell by using five control points and varying the radius (width) along the height (in total five optimization variables).

By increasing the variables and using five control points and varying radius(width), angle, length factor, and sharpness factor, to achieve gravity balancing for a higher target window, a rather balanced profile can be obtained with a straight line up until 140 degrees, which is shown in Figure 2.13 (a) and (b) shows the corresponding geometry.

2.3.3. EXPERIMENTAL MEASUREMENTS

Two 3D-printed prototypes are used for the experimental measurement, both corresponding to simulation with material properties of Tough 1500. The prototype seen in Figure 2.5 (a) represents the default L-shape helicoidal shell joint with the set geometric values seen in Table 2.2 and (b) is the CAD model corresponding to the helicoidal L-shape prototype optimized for a 90-degree window using the global geometric optimization with six optimization variables and adjusted bounds for limitations of manufacturing and testing. Table 2.3 includes the geometric parameters used for the design of this prototype.

Figure 2.14 (a) shows the output profile of the default L-shape helicoidal shell joint and (b) shows the normalized profile. Figure 2.15 (a) shows the output profile of the optimized L-shape helicoidal shell joint for the 90-degree target window and (b) shows the corresponding normalized moment. Figure 2.16 shows the picture of the default L-shape prototype getting twisted in different stages. It can be observed from both these prototypes that while the prototype conforms to the same behavior, as evident from the normalized output, the actual output deviates from the simulation, by showing a softer structure, showing less resistance to being twisted.

2.4. DISCUSSION

Although an analytic model was not developed in this study, the effect of geometric parameters on the L-shape helicoidal shell mechanism was observed through finite element simulation. This study com-

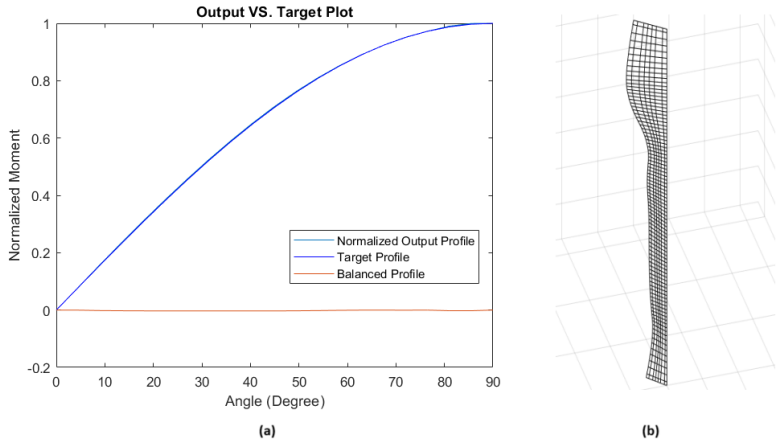

Figure 2.11.: (a) The optimized torque-angle profile for the base helicoidal shell, based on variation of radius (width) and angle with ten control points for 90 degrees and (b) The corresponding optimized geometry

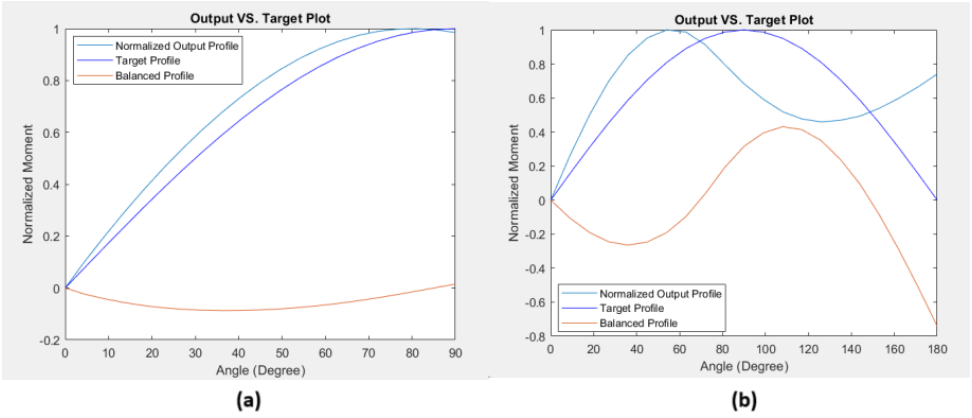

Figure 2.12.: The optimized torque-angle profile for the L-shape helicoidal shell that is based on the variation radius (width) along the height for a) 90, b) 180 degrees.

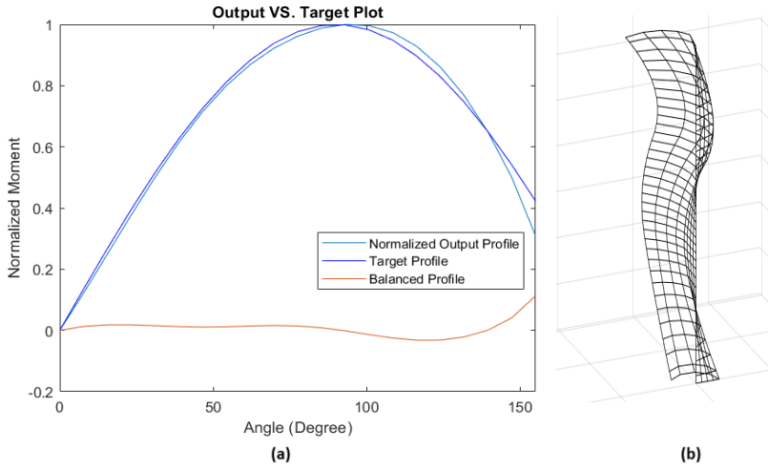

Figure 2.13.: The optimized torque-angle profile for the L-shape helicoidal shell in the target window of 180 degrees, based on the variation of radius (width), angle, L_f, and S_f b) The corresponding optimized geometry

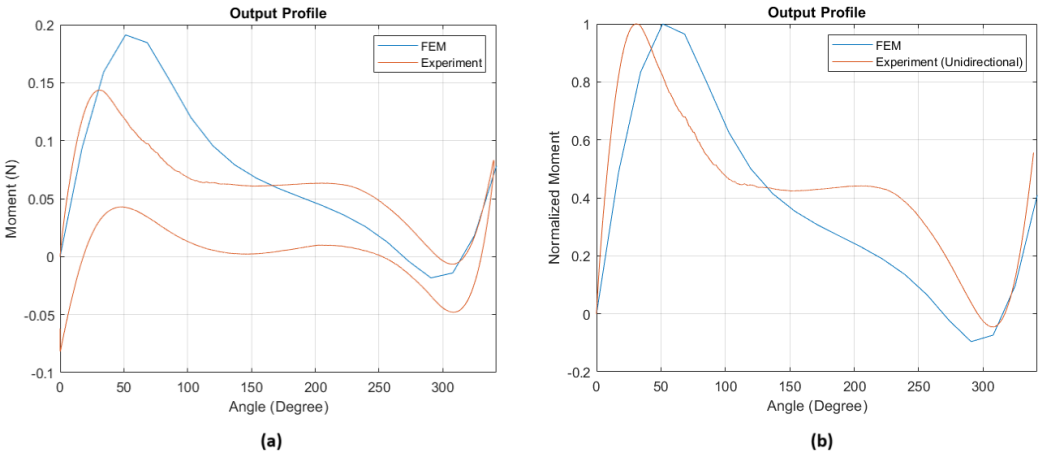

Figure 2.14.: (a) Output profile of default L-shape prototype: FEM VS. experimental data and (b) Normalized moment

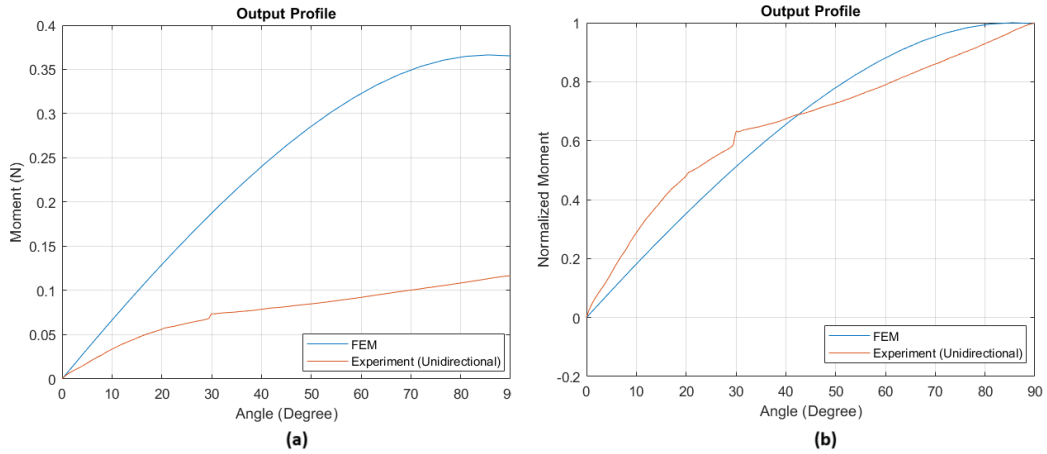

Figure 2.15.: (a) Output profile of optimized L-shape prototype for 90 degrees: FEM VS. experimental data and (b) Normalized moment

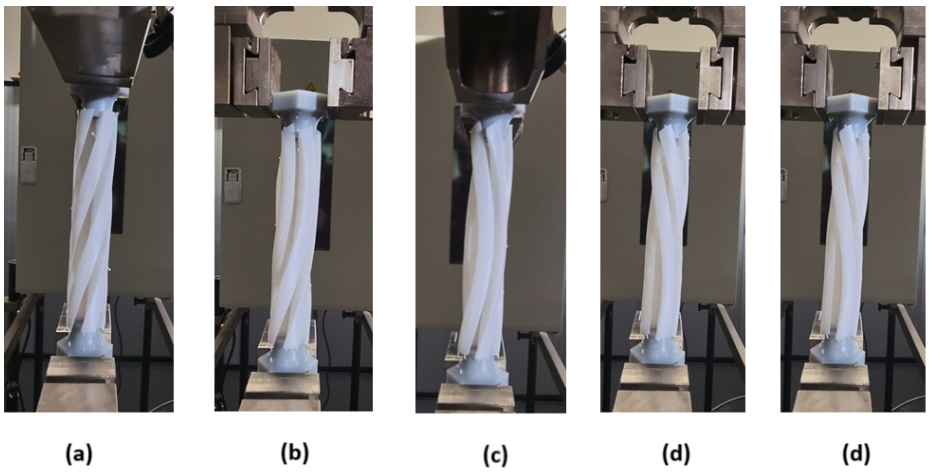

Figure 2.16.: Default L-shape design deformation: (a) Initial position (b) 90 degrees (c) 180 degrees (d) 270 degrees (e) 340 degrees

Table 2.3.: Optimization parameters for 3D printed Prototype

Parameter	Value
T (Thickness)	0.0005[m]
W (Width)	0.0066[m]
P (Pitch)	0.1040[m]
H (Height)	0.0727[m]
L_f	0.9274
S_f	1.1592

menced with an understanding of the hybrid behavior of the L-shape helicoidal shell where the structure can behave more similarly to the base helicoidal shell or deform as a whole when external force is applied. This alternating behavior is heavily influenced by the length factor and the sharpness factor as these two parameters affect the key difference between the above-mentioned design variants: the flange. This means a less wide flange and a less sharp flange lead to behavior closer to the base helicoidal shell, and the larger flange and the sharper it is, triggers the bistability and the negative stiffness region between the two stable points.

The global geometric parameters approach is very useful to find a starting point for finer optimization through local geometric adjustment as these parameters affect the whole structure, however, due to the lack of local control, its ability to manipulate the nonlinear behavior of the helicoidal shell is limited. With that said, if local geometric parameter adjustment is also used, a satisfactory balanced profile can be achieved.

As for the base helicoidal shell, it can be observed that by controlling local parameters a very well-balanced gravity-balancing profile can be optimized for a 90-degree angle window, however, exceeding this window, does not result in balanced profiles, as this structure does not exhibit bistability and hence the possibility of a negative stiffness region. To make the balanced profile even more enhanced, increasing the number of control points is key. This was shown by the enhanced balanced profile from five control points to ten control points.

For the L-shape helicoidal shell, recreating a gravity-balanced profile with global geometric parameters approach until 90 degrees is accessible, however, this approach is not enough to produce gravity-balanced profiles for larger angle windows. The result of the local geometric optimization approach for the L-shape design is promising and shows an ideal balanced profile up to 140 degrees. However, even both the approaches used in this study were unable to achieve a full 180-degree gravity-balanced profile which shows the limitation of optimizing of a single shell.

The experimental results show a rather considerable difference in the actual resisting moment of this structure. The material used for the prototype studied in this paper is highly viscoelastic, and its behavior changes over time. Additionally, the type of resin used for this printing method is very dependent on the curing procedure, time, and temperature [31], and if any of these parameters are somewhat changed, the properties of this material are altered, which can be a hypothetical reason for this disparity.

2.5. CONCLUSION

In this study, we conducted a comprehensive investigation into the geometric analysis, optimization, and experimental validation of a novel helicoidal shell design studied by Radaelli [5], particularly focusing on developing an L-shape variant of this structure. The intricate relationship between geometric parameters and the resulting torque-angle profile was explored through both global and local optimization approaches, shedding light on the challenges and opportunities in tailoring compliant joint behavior.

The impact of parameters such as thickness, width, pitch, height, length factor, and sharpness factor on the torque-angle profile was analyzed in detail. These insights served as a foundation for the subsequent optimization efforts, revealing the complex interplay of these factors in achieving desired joint behaviors.

While the bistable behavior shows a potential for profiles emulating a sine function, reaching a total sine function with the presented approaches in the study was only realized up until 140 degrees and larger angle windows remain an intriguing prospect to be studied. As this structure consists of a number of similar shells, the behavior is limited to the profile exhibited by each shell. However, by making a more complex algorithm, and optimizing two or more shells simultaneously (for example, optimizing a cross-section like a Z-shape), more control is achieved on the torque-angle profile. An even more complex optimization algorithm can be developed to optimize separate shells (with separate thicknesses). This shows potential for recreating a larger range of nonlinear torque-angle profiles, and not only the possibility of achieving gravity-balancing for a larger angle window but also the possibility of achieving potentially a neutrally stable joint.

Furthermore, more complex optimization does not always lead to better results as the search domain gets larger and the possibility of reaching a local minimum instead of a global minimum increases. Developing optimization with multiple starting points can be a promising solution for this possible error.

Additionally, this study was first carried out through simulation and numerical analysis and then experimental validations were undertaken by considering the limitations of manufacturing and testing. This study can start from the fabrication, and then enhance the numerical model to correctly predict the behavior, by taking into account the proper material models. The fabrication of prototypes, especially, with the goal of reducing the stress concentrations, is another suggestion for future studies.

REFERENCES

[1] S. Hampali, A. P. S, and G. K. Ananthasuresh. "A Tunable Variable-Torque Compliant Hinge Using Open-Section Shells". In: *Journal of Mechanisms and Robotics* 12.6 (Dec. 2020). DOI: 10.1115/1.4047440.

[2] G. Radaelli and J. L. Herder. "Gravity balanced compliant shell mechanisms". In: *International Journal of Solids and Structures* 118-119 (July 2017), pp. 78–88. DOI: 10.1016/j.ijsolstr.2017.04.021. URL: https://doi.org/10.1016/j.ijsolstr.2017.04.021.

[3] K. A. Seffen. "Compliant shell mechanisms". In: *Philosophical Transactions of the Royal Society A* 370.1965 (Apr. 2012), pp. 2010–2026. DOI: 10.1098/rsta.2011.0347. URL: https://doi.org/10.1098/rsta.2011.0347.

[4] J. Stacey. "Composite compliant shell mechanisms: Tailoring and characterisation". PhD thesis. University of Bristol, 2021.

[5] G. Radaelli. "Reverse-twisting of helicoidal shells to obtain neutrally stable linkage mechanisms". In: *International Journal of Mechanical Sciences* 202-203 (July 2021), p. 106532. DOI: 10.1016/j.ijmecsci.2021.106532. URL: https://doi.org/10.1016/j.ijmecsci.2021.106532.

[6] H. N. Prakashah and H. Zhou. "Synthesis of Constant Torque Compliant Mechanisms". In: *Journal of Mechanisms and Robotics* 8.6 (Aug. 2015). DOI: 10.1115/1.4034885.

[7] C.-W. Hou and C.-C. Lan. "Functional joint mechanisms with constant-torque outputs". In: *Mechanism and Machine Theory* 62 (Apr. 2013), pp. 166–181. DOI: 10.1016/j.mechmachtheory.2012.12.002. URL: https://doi.org/10.1016/j.mechmachtheory.2012.12.002.

[8] *Novel Design of a Passive Variable Stiffness Joint Mechanism: Inspiration From Biomechanics of Hand Joints*. Vol. Volume 2: Control, Monitoring, and Energy Harvesting of Vibratory Systems; Cooperative and Networked Control; Delay Systems; Dynamical Modeling and Diagnostics in Biomedical Systems; Estimation and Id of Energy Systems; Fault Detection; Flow and Thermal Systems; Haptics and Hand Motion; Human Assistive Systems and Wearable Robots; Instrumentation and Characterization in Bio-Systems; Intelligent Transportation Systems; Linear Systems and Robust Control; Marine Vehicles; Nonholonomic Systems. Dynamic Systems and Control Conference. Oct. 2013, V002T28A003. DOI: 10.1115/DSCC2013-3980. eprint: https://asmedigitalcollection.asme.org/DSCC/proceedings-pdf/DSCC2013/56130/V002T28A003/4444656/v002t28a003-dscc2013-3980.pdf. URL: https://doi.org/10.1115/DSCC2013-3980.

[9] S. Hampali, P. Anoosha, and G. K. Ananthasuresh. *An Open-Section Shell Designed for Customized Bending and Twisting to Ease Sitting and Rising in a Chair*. Springer Nature, Jan. 2019. DOI: 10.1007/978-981-10-8597-0\{_}36.

[10] A. A. Nobaveh, J. L. Herder, and G. Radaelli. "A compliant Continuously Variable Transmission (CVT)". In: *Mechanism and Machine Theory* 184 (June 2023), p. 105281. DOI: 10.1016/j.mechmachtheory.2023.105281. URL: https://doi.org/10.1016/j.mechmachtheory.2023.105281.

[11] H.-T. Pham and D.-A. Wang. "A constant-force bistable mechanism for force regulation and overload protection". In: *Mechanism and Machine Theory* 46.7 (July 2011), pp. 899–909. DOI: 10.1016/j.mechmachtheory.2011.02.008. URL: https://doi.org/10.1016/j.mechmachtheory.2011.02.008.

[12] R. Barents, M. Schenk, W. D. Van Dorsser, B. M. Wisse, and J. L. Herder. "Spring-to-Spring balancing as Energy-Free adjustment method in gravity equilibrators". In: *Journal of Mechanical Design* 133.6 (June 2011). DOI: 10.1115/1.4004101. URL: https://doi.org/10.1115/1.4004101.

[13] H.-C. Hsieh, L. Chien, and C.-C. Lan. "Mechanical design of a gravity-balancing wearable exoskeleton for the motion enhancement of human upper limb". In: *IEEE Transactions on Neural Systems and Rehabilitation Engineering* 12.2 (May 2015). DOI: 10.1109/icra.2015.7139893. URL: https://doi.org/10.1109/icra.2015.7139893.

[14] S. K. Agrawal and A. Fattah. "Theory and design of an orthotic device for full or partial gravity-balancing of a human leg during motion". In: *IEEE Transactions on Neural Systems and Rehabilitation Engineering* 12.2 (June 2004), pp. 157–165. DOI: 10.1109/tnsre.2004.827221. URL: https://doi.org/10.1109/tnsre.2004.827221.

[15] S. K. Agrawal and A. Fattah. "Gravity-balancing of spatial robotic manipulators". In: *Mechanism and Machine Theory* 39.12 (Dec. 2004), pp. 1331–1344. DOI: 10.1016/j.mechmachtheory.2004.05.019. URL: https://doi.org/10.1016/j.mechmachtheory.2004.05.019.

[16] K. Koser. "A cam mechanism for gravity-balancing". In: *Mechanics Research Communications* 36.4 (June 2009), pp. 523–530. DOI: 10.1016/j.mechrescom.2008.12.005. URL: https://doi.org/10.1016/j.mechrescom.2008.12.005.

[17] M. Tschiersky, E. E. Hekman, D. M. Brouwer, and J. L. Herder. "Gravity balancing flexure springs for an assistive elbow orthosis". In: *IEEE transactions on medical robotics and bionics* 1.3 (Aug. 2019), pp. 177–188. DOI: 10.1109/tmrb.2019.2930341. URL: https://doi.org/10.1109/tmrb.2019.2930341.

[18] M. Tschiersky, E. E. Hekman, J. L. Herder, and D. M. Brouwer. "Gravity balancing flexure spring mechanisms for shoulder support in assistive orthoses". In: *IEEE transactions on medical robotics and bionics* 4.2 (May 2022), pp. 448–459. DOI: 10.1109/tmrb.2022.3155293. URL: https://doi.org/10.1109/tmrb.2022.3155293.

[19] B. P. Trease, Y.-M. Moon, and S. Kota. "Design of Large-Displacement Compliant Joints". In: *ASME Digital Collection* (Nov. 2004). DOI: 10.1115/1.1900149. URL: https://doi.org/10.1115/1.1900149.

[20] Z. W. Yang and C.-C. Lan. "An adjustable gravity-balancing mechanism using planar extension and compression springs". In: *Mechanism and Machine Theory* 92 (Oct. 2015), pp. 314–329. DOI: 10.1016/j.mechmachtheory.2015.05.006. URL: https://doi.org/10.1016/j.mechmachtheory.2015.05.006.

[21] D. Franchetti, G. Boschetti, and B. Lenzo. "Passive Gravity Balancing with a Self-Regulating Mechanism for Variable Payload". In: *Machines* 9.8 (July 2021), p. 145. DOI: 10.3390/machines9080145. URL: https://doi.org/10.3390/machines9080145.

[22] Y. R. Chheta, R. Joshi, K. K. Gotewal, and M. ManoahStephen. "A review on passive gravity compensation". In: *2017 International conference of Electronics, Communication and Aerospace Technology (ICECA)* (Apr. 2017). DOI: 10.1109/iceca.2017.8203668. URL: https://doi.org/10.1109/iceca.2017.8203668.

[23] V. L. Nguyen, C.-H. Kuo, and P. T. Lin. "Reliability-Based analysis and optimization of the gravity balancing performance of Spring-Articulated serial robots with uncertainties". In: *Journal of Mechanisms and Robotics* 14.3 (Dec. 2021). DOI: 10.1115/1.4053048. URL: https://doi.org/10.1115/1.4053048.

[24] W.-B. Lee, S.-D. Lee, and J.-B. Song. "Design of a 6-DOF collaborative robot arm with counterbalance mechanisms". In: *IEEE International Conference on Robotics and Automation (ICRA)* (May 2017). DOI: 10.1109/icra.2017.7989425. URL: https://doi.org/10.1109/icra.2017.7989425.

[25] G. Carpino, D. Accoto, M. Di Palo, N. L. Tagliamonte, F. Sergi, and E. Guglielmelli. "Design of a rotary passive viscoelastic joint for wearable robots". In: *IEEE International Conference on Rehabilitation Robotics* (June 2011). DOI: 10.1109/icorr.2011.5975356. URL: https://doi.org/10.1109/icorr.2011.5975356.

[26] S. Wolf, O. Eiberger, and G. Hirzinger. "The DLR FSJ: Energy based design of a variable stiffness joint". In: *IEEE International Conference on Robotics and Automation* (May 2011). DOI: 10.1109/icra.2011.5980303. URL: https://doi.org/10.1109/icra.2011.5980303.

[27] D. Accoto, N. L. Tagliamonte, G. Carpino, F. Sergi, M. Di Palo, and E. Guglielmelli. "pVEJ: A modular passive viscoelastic joint for assistive wearable robots". In: *Proceedings—IEEE International Conference on Robotics and Automation* (May 2012). DOI: 10.1109/icra.2012.6225167. URL: https://doi.org/10.1109/icra.2012.6225167.

[28] A. P. Nagy, S. T. IJsselmuiden, and M. Abdalla. "Isogeometric design of anisotropic shells: Optimal form and material distribution". In: *Computer Methods in Applied Mechanics and Engineering* 264 (2011), pp. 145–162. DOI: 10.1016/j.cma.2013.05.019. URL: https://doi.org/10.1016/j.cma.2013.05.019.

[29] *Tough 1500 Datasheet*. URL: https://formlabs-media.formlabs.com/datasheets/Tough_1500_TDS_EN.pdf.

[30] *Form 3+: Industrial-Quality Desktop Resin 3D Printer*. URL: https://formlabs.com/eu/3d-printers/form-3/.

[31] *Formlabs Material Library*. URL: https://formlabs-media.formlabs.com/filer_public/ac/89/ac8963db-f54a-4cac-8fe9-fb740a7b06f1/formlabs-materials-library.pdf.

3

CONCLUSION

This study investigated the possibility of synthesizing nonlinear torque-angle profiles using helicoidal shell joints by analyzing different design variants and developing an L-shape design with bistable behavior. The primary focus of this research was introducing a gravity-balancing profile and it was shown that with the methods and design variants proposed in this study, an adequate gravity-balancing profile up until 140 degrees was achievable. Two optimization approaches were utilized and the results of them were presented. Additionally, CAD models and prototypes were developed to provide a link between simulation and the real behavior of the models. The strengths and limitations of the approaches presented as well as the limits of the studied structures were presented and discussed. Furthermore, the differences and disparity between simulation and experimental results were presented and analyzed. This study concluded with suggestions for further research and methods to enhance gravity-balancing using helicoidal shell joints.

The author of this thesis proposes further study of this compliant shell mechanism for achieving gravity-balancing profiles with larger angle windows as well as synthesizing alternative nonlinear torque-angle profiles, such as neutrally stable profiles. Additionally, an application-based approach can enhance this study by synthesizing nonlinear torque-angle profiles using the methodology presented in this research for engineering applications, such as gravity-balancing medical devices and structures in the field of biomechanical design. This study showed the potential of helicoidal shells for designing compliant joints, however, this potential should also be studied for implementation and practical use.

Furthermore, developing a functional joint is beyond the possible nonlinear profiles obtained by simulations, or even one-time experimental measurements. The effects of fatigue and creep can significantly affect the functionality of a joint, as the question arises whether the obtained nonlinear behavior is repeatable. Additionally, putting the result of this research to good use, requires a detailed study of fabrication methods and materials, to provide adequate mechanical behaviors in joints made for engineering applications. This also requires enhancing the numerical methodology by taking into account the nonlinearities of the materials as well as using alternatives to linear-elastic models to simulate more precise results.

A

THEORETICAL BACKGROUND

This appendix will provide a brief introductory overview of the main theoretical foundations that worked as the underlying basis for the numerical methodology employed in this thesis. Additionally, further resources will be recommended to interested readers.

A.1. ISOGEOMETRIC ANALYSIS AND NURBS

Isogeometric analysis (IGA) is a relatively recent technology in computational mechanics that enables the integration of Finite Element Analysis (FEA) and Computer-Aided Design (CAD) into a unified process. This has significant implications for practical engineering design scenarios, reducing the time from design to analysis and resulting in notable efficiency gains. Some key advantages of IGA over traditional Finite Element Methods (FEM) include [1]:

- IGA utilizes NURBS (Non-Uniform Rational B-Splines), a type of spline commonly used in CAD, as its basic function for analysis. This eliminates the need for time-consuming and error-prone meshing, allowing the exact representation of complex geometries.
- IGA eliminates the requirement for re-meshing when there are changes in geometry, which is particularly advantageous in applications such as fluid dynamics.
- IGA can address a broader range of problems compared to traditional FEM, including those involving high-order derivatives.
- IGA is recognized for its higher accuracy when using the same degree of polynomial approximation as traditional FEM.

The procedure used in IGA can be summarized as follows [2]:

- A CAD model of the problem domain is created.
- The CAD model is converted into a mesh of NURBS (Non-Uniform Rational B-Splines) control points.
- The NURBS control points are used to define the basis functions for the IGA solution.
- The PDEs governing the problem are solved using the IGA basis functions.
- The solution is then used to obtain the desired engineering results, such as stresses, strains, and displacements.

It should be noted that in isogeometric analysis (IGA), a CAD model is typically utilized as the starting point for the analysis. However, IGA itself is not responsible for creating the CAD model. Instead, it leverages the existing CAD model of the problem domain. The general workflow in IGA involves taking the CAD model, which represents the geometric details of the structure or object, and converting it into a mesh of Non-Uniform Rational B-Splines (NURBS) control points. This conversion allows IGA to seamlessly integrate the geometric representation with the mathematical framework used for analysis.

NURBS, or Non-Uniform Rational B-Splines, are mathematical representations commonly used in computer-aided design (CAD) and computer graphics. They provide a flexible and precise way to represent curves and surfaces, making them an essential tool in geometric modeling. NURBS-based geometry is the application of NURBS curves and surfaces to define shapes and surfaces in digital design and engineering.

B-Splines are a type of mathematical curve that uses piecewise-defined polynomial functions to interpolate or approximate points in space. They are defined by control points and basis functions. NURBS (Non-Uniform Rational B-Splines) are a type of mathematical function that is used in computer-aided design (CAD) to represent curves and surfaces. NURBS are a generalization of B-Splines, which were first introduced by mathematician Carl Friedrich Gauss in the 18th century [1].NURBS can represent a wider variety of curves and surfaces, including conic sections such as circles and ellipses, which cannot be represented exactly by B-Splines. NURBS are more efficient to evaluate and refine than B-Splines. The "non-uniform" aspect means that the spacing between control points is not necessarily uniform. This allows for more flexibility in shaping curves and surfaces. The "rational" part refers to the fact that NURBS curves and surfaces use rational functions. Each control point has an associated weight, allowing for additional control over the shape. NURBS are used in various applications, including computer-aided design (CAD), computer-aided manufacturing (CAM), and computer graphics. NURBS are also used in the automotive, aerospace, and shipbuilding industries to design complex parts [1]. NURBS are used to model everything from automobile bodies and ship hulls to animated characters in the latest feature-length film. To fully exploit the flexibility of NURBS, a thorough working knowledge of the underlying mathematics is necessary [3]. NURBS are also used as the basis functions in isogeometric analysis because they offer some advantages over traditional finite element basis functions, including [4]:

- Flexibility: NURBS are capable of representing complex geometries with ease.
- Accuracy: NURBS are very accurate, even for high-order problems.
- Discontinuity control: NURBS basis functions can be discontinuous across element boundaries, which can be beneficial for certain applications.
- Convergence: NURBS-based methods are known to converge rapidly, even for problems with complex geometries.

In addition to these advantages, as NURBS are the basis functions of choice in many CAD systems, this makes them a natural choice for isogeometric analysis, as it eliminates the need to convert between different types of basis functions.

NURBS curves are defined by a set of control points and associated weights. The curve smoothly passes through these control points, and the weights determine the influence of each control point on the curve's shape. The degree of the curve indicates the order of the polynomial functions used. NURBS surfaces extend the concept of NURBS curves into two

dimensions. They are defined by a grid of control points in both the u- and v-directions, each with an associated weight. The weights provide additional control over the shape and surface properties. NURBS-based geometry provides a precise and flexible way to represent complex shapes. The ability to control the degree, weights, and arrangement of control points allows for the creation of a wide variety of shapes, from simple to highly intricate. NURBS can be used for both interpolation (passing through specified points) and approximation (fitting a curve or surface to given data). This versatility makes them suitable for various design applications.

For a more in-depth exploration of Isogeometric Analysis and NURBS, readers are encouraged to consult the recommended references[1–6].

A.2. KIRCHHOFF–LOVE PLATE THEORY

Kirchhoff-Love Theory is a fundamental principle in the field of plate theory, providing a set of equations that describe the behavior of thin plates under various loads. The Kirchhoff plate theory or classical plate theory (CPT) is an extension of the Euler–Bernoulli beam theory to plates. Kirchhoff-Love theory was developed by Augustus Edward Hough Love in 1888, using the ideas of Gustav Kirchhoff. It is based on the assumption that straight lines perpendicular to the mid-surface (i.e., transverse normals) before deformation remain straight after deformation. The Kirchhoff hypothesis consists of the following three parts [7]:

1) Straight lines perpendicular to the mid-surface (i.e., transverse normals) before deformation remain straight after deformation.

2) The transverse normals do not experience elongation (i.e., they are inextensible).

3) The middle surface of the plate is in a state of plane stress.

The main equations of Kirchhoff-Love Theory describe the relationships between the moments, shears, and bending moments in terms of the plate deflections. The theory is widely used in engineering and physics to analyze the behavior of structures such as beams and plates under various loading conditions. It's important to note that while Kirchhoff's Love Theory is suitable for thin plates, it may not be accurate for thick plates, and more advanced theories, such as the Mindlin-Reissner theory, are used in those cases. It is also not valid for plates with large deflections, shear deformations, or thickness variations. Detailed formulation of this theory can be found in [7].

REFERENCES

[1] V. P. Nguyen, C. Anitescu, S. P. A. Bordas, and T. Rabczuk. "Isogeometric analysis: An overview and computer implementation aspects". In: *Mathematics and Computers in Simulation* 117 (Nov. 2015), pp. 89–116. DOI: 10.1016/j.matcom.2015.05.008. URL: https://doi.org/10.1016/j.matcom.2015.05.008.

[2] T. J. Hughes, J. A. Cottrell, and Y. Bazilevs. "Isogeometric analysis: CAD, finite elements, NURBS, exact geometry and mesh refinement". In: *Computer Methods in Applied Mechanics and Engineering* 194.39-41 (Oct. 2005), pp. 4135–4195. DOI: 10.1016/j.cma.2004.10.008. URL: https://doi.org/10.1016/j.cma.2004.10.008.

[3] D. F. Rogers. *An introduction to NURBS*. Morgan Kaufmann, Jan. 2001.

[4] J. A. Cottrell, T. J. R. Hughes, and Y. Bazilevs. *Isogeometric analysis: Toward Integration of CAD and FEA*. John Wiley & Sons, Aug. 2009.

[5] E. H. Van Brummelen, C. Vuik, M. Möller, C. V. Verhoosel, B. Simeon, and B. Jüttler. *ISOGeometric Analysis and Applications 2018*. Jan. 2021. DOI: 10.1007/978-3-030-49836-8. URL: https://doi.org/10.1007/978-3-030-49836-8.

[6] A. P. Nagy, S. T. IJsselmuiden, and M. Abdalla. "Isogeometric design of anisotropic shells: Optimal form and material distribution". In: *Computer Methods in Applied Mechanics and Engineering* 264 (2011), pp. 145–162. DOI: 10.1016/j.cma.2013.05.019. URL: https://doi.org/10.1016/j.cma.2013.05.019.

[7] J. N. Reddy. *Theory and analysis of elastic plates and shells*. Nov. 2006. DOI: 10.1201/9780849384165. URL: https://doi.org/10.1201/9780849384165.

B

Alternative Designs

B.1. Design Modification Approach

To explore the potential nonlinear torque-angle profiles, three main approaches were initially utilized to modify the original compliant helicoidal shell mechanism studied by Radaelli [1]. These approaches are described below.

- Applying mathematical functions to the outer edge of the helicoidal shell: In this approach, different mathematical functions such as taper, polynomial (2^{nd}, 3^{rd}, and 4^{th} degree), and cosine function with different periods were implemented as and the resulting torque-angle profile was observed. In other words, instead of a constant width, $w = w(z)$ is used as a varying width. Another approach utilized in this research based on applying mathematical functions is developing a double-sided model (with the middle edge constrained) and applying different mathematical functions to each side such as $w_1 = w_1(z)$ and $w_2 = w_2(z)$.

- Applying different cross-sections to the helicoidal shell: The inspiration for this approach was testing the common cross-section shapes that can be seen in beams. An example can be seen in Figure B.1. L-shape, C-shape, Z-shape, and T-shape cross sections are developed for the helicoidal shell in this study and the resulting torque-angle profile is observed. To create these cross sections, a curved flange was designed based on the cylindrical coordinates, therefore, the flange is shaped as a circular arc. To control the shape of this flange, two geometrical factors were created, length factor (L_f) and sharpness factor (S_f). The length factor is the ratio of the flange length (arc length) to the width of the shell (web length), and the sharpness factor is defined as the ratio between the radius of the endpoint of the arc at θ_{arc} where θ_{arc} is the arc angle and the width of the shell (web length). In theory, the minimum value for the length factor can be as low as zero which is the simple helicoidal shell that does not have an additional flange, and the minimum value for the sharpness factor is one, as the minimum radius of any point on the arc is the same as the shell width. The control points on the flange starting from the endpoint of the web to the endpoint of the arc at θ_{arc}, are defined linearly varying from w to $Sh_f \times w$. A higher value for the sharpness factor translates to a less sharp L-shape. Figure B.2 depicts the Finite Element Model (FEM) for each of the implemented cross-sections.

- Applying varying pitch to the helicoidal shell: While the original helicoidal shell structure has a constant pitch, varying pitch values for the helicoidal shell are studied in this research to observe their effect. This includes having linearly increasing or decreasing

B

pitch along the shell's height so that pitch would be $p = p(z)$, half helix shape (utilizing both negative and positive pitch in the lower and upper half of the helicoidal shell). Figure B.3 shows the finite element model as an example of varying pitch, where the pitch goes from positive to negative at the middle of the helicoidal shell.

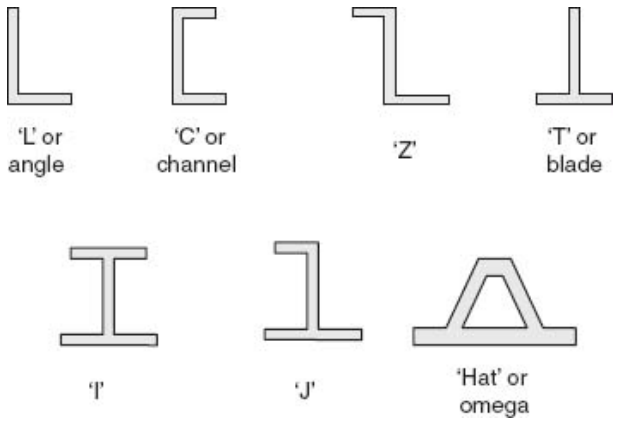

Figure B.1.: Typical cross-sections in beams [2].

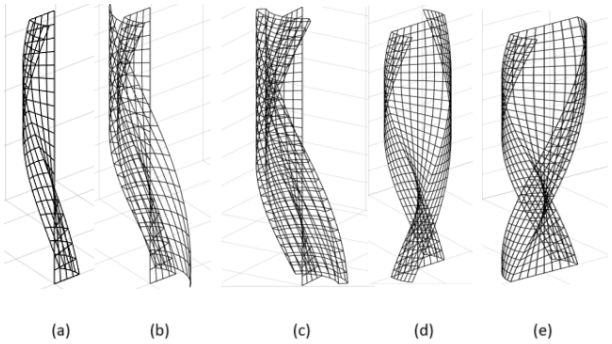

Figure B.2.: Finite Element Models for different cross sections: (a) L-shape (b) T-shape: Type I (c) T-shape: Type II (d) Z-shape (e) C-shape.

REFERENCES

[1] G. Radaelli. "Reverse-twisting of helicoidal shells to obtain neutrally stable linkage mechanisms". In: *International Journal of Mechanical Sciences* 202-203 (July 2021), p. 106532. DOI: 10.1016/j.ijmecsci.2021.106532. URL: https://doi.org/10.1016/j.ijmecsci.2021.106532.

[2] C. Kassapoglou. *Design and Analysis of Composite Structures: With Applications to Aerospace Structures, 2nd edition*. URL: https://www.oreilly.com/library/view/design-and-analysis/9781118536940/OEBPS/9781118536940_epub_c_08.htm.

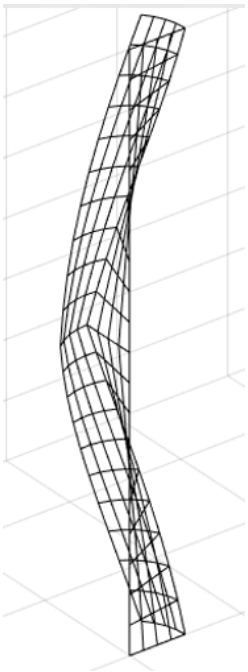

Figure B.3.: Half-helix design for helicoidal shell

C

SUPPLEMENTARY OPTIMIZATION RESULTS

This appendix includes supplementary optimization results for the main paper as well as the results included in the main paper in one place. These results can provide further insights into how different combinations in optimization can show different levels of tunability in the structure.

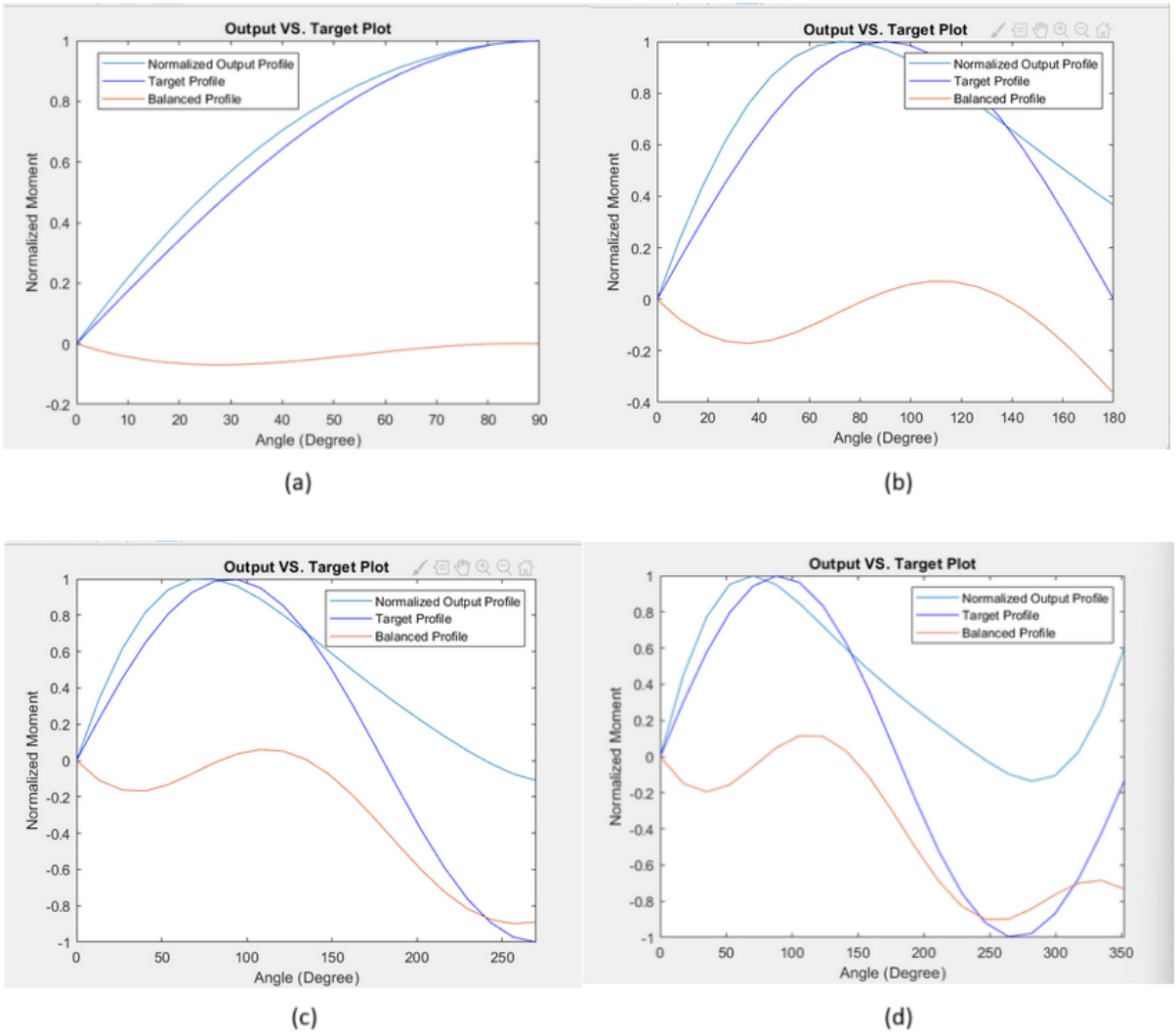

Figure C.1.: The optimized torque-angle profile, based on the variation of L_f and S_f for a) 90, b) 180, c) 270 d) 360 degrees.

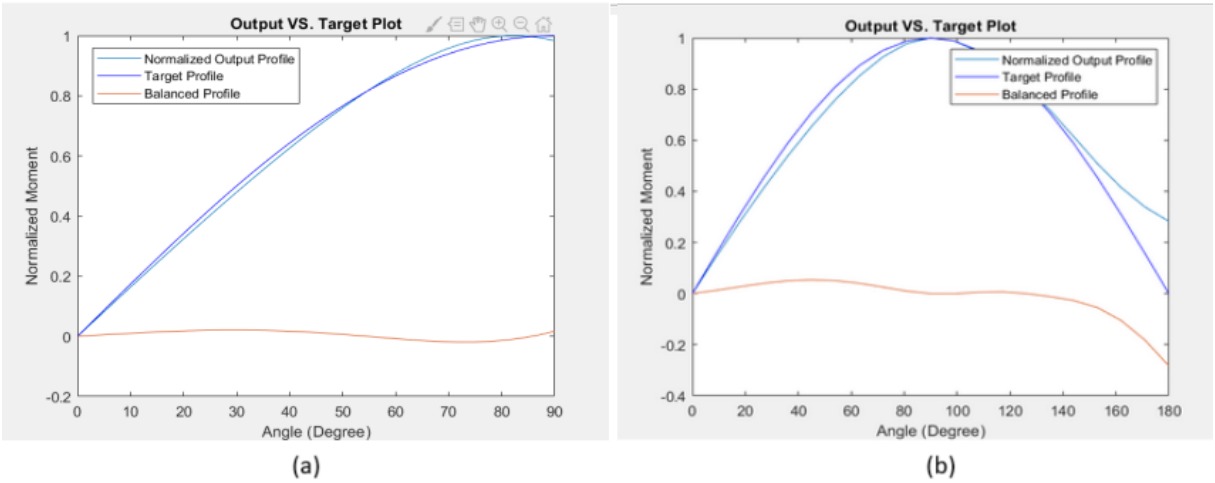

Figure C.2.: The optimized torque-angle profile, based on the variation of all six geometric variables for a) 90, b) 180 degrees.

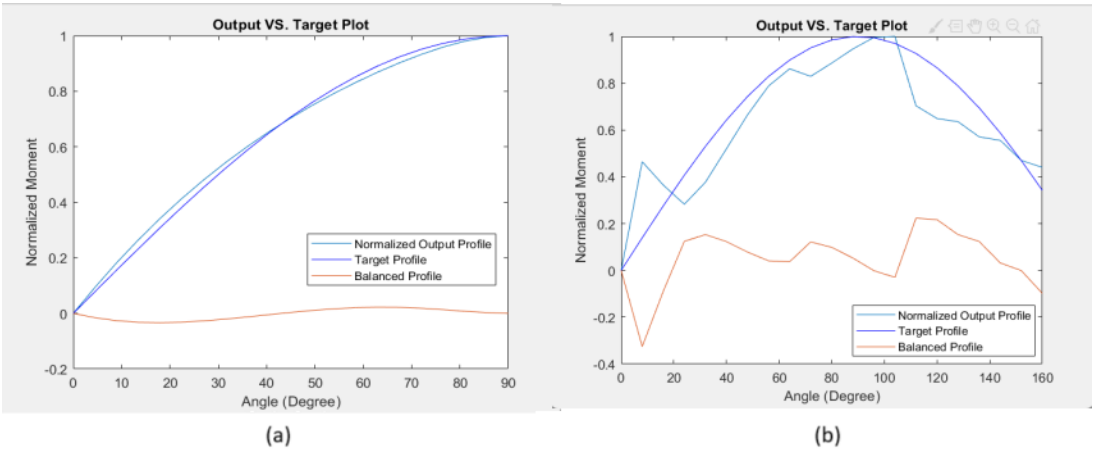

Figure C.3.: The optimized torque-angle profile for the base helicoidal shell, based on the variation radius (width) along the height for a) 90, b) 180 degrees.

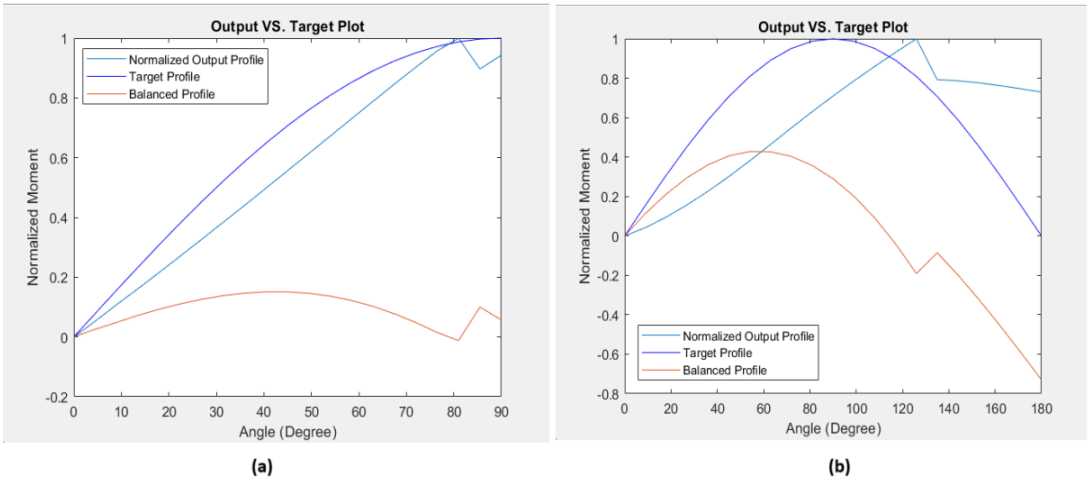

Figure C.4.: The optimized torque-angle profile for the base helicoidal shell, based on the variation radius and angle along the height for a) 90, and b) 180 degrees.

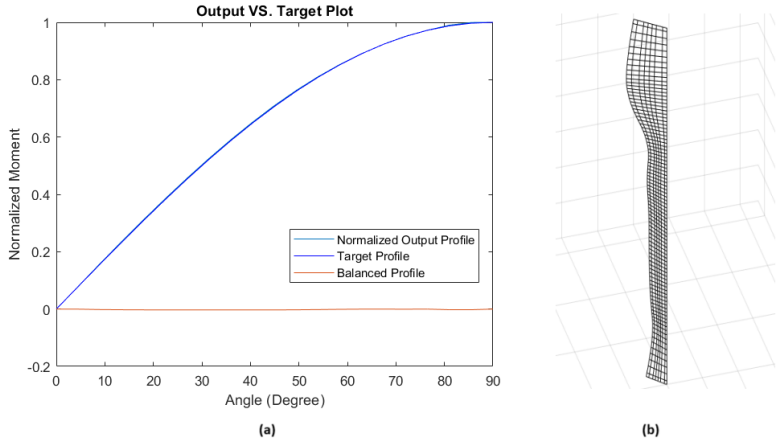

Figure C.5.: (a) The optimized torque-angle profile for the base helicoidal shell, based on variation of radius (width) and angle with ten control points for 90 degrees and (b) The corresponding optimized geometry

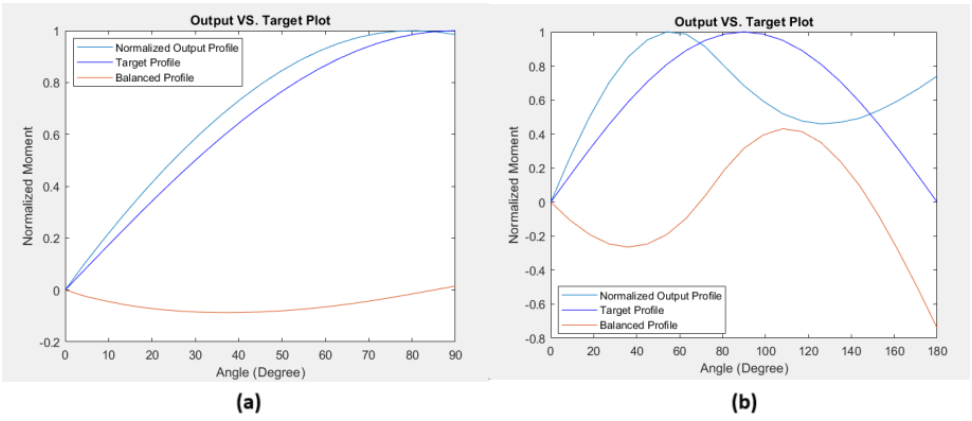

Figure C.6.: The optimized torque-angle profile for the L-shape helicoidal shell that is based on the variation radius (width) along the height for a) 90, b) 180 degrees.

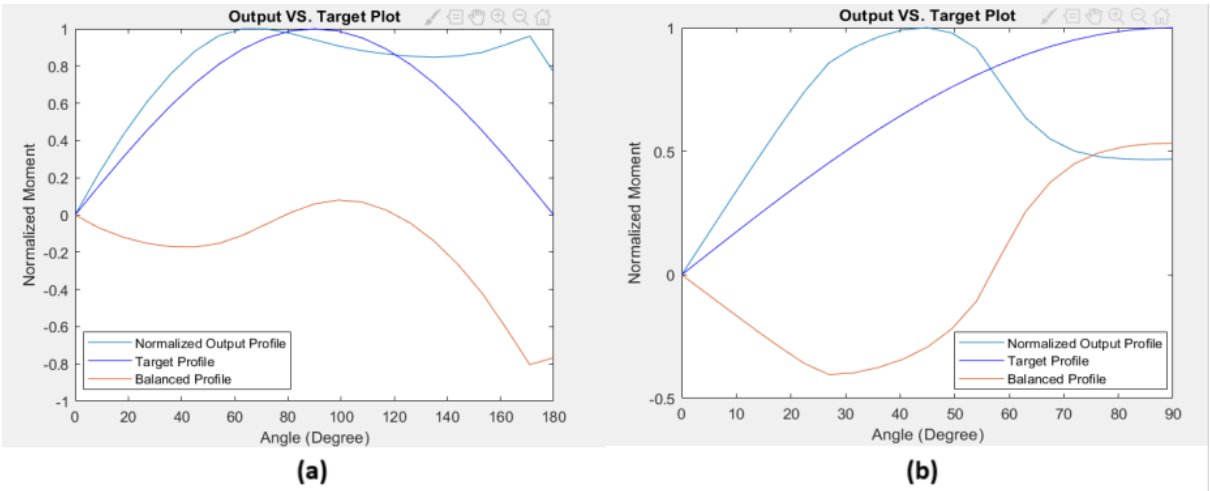

Figure C.7.: The optimized torque-angle profile for the L-shape helicoidal shell in the target window of 180 degrees that is based on the variation of radius and a) length factor, b) sharpness factor along the height.

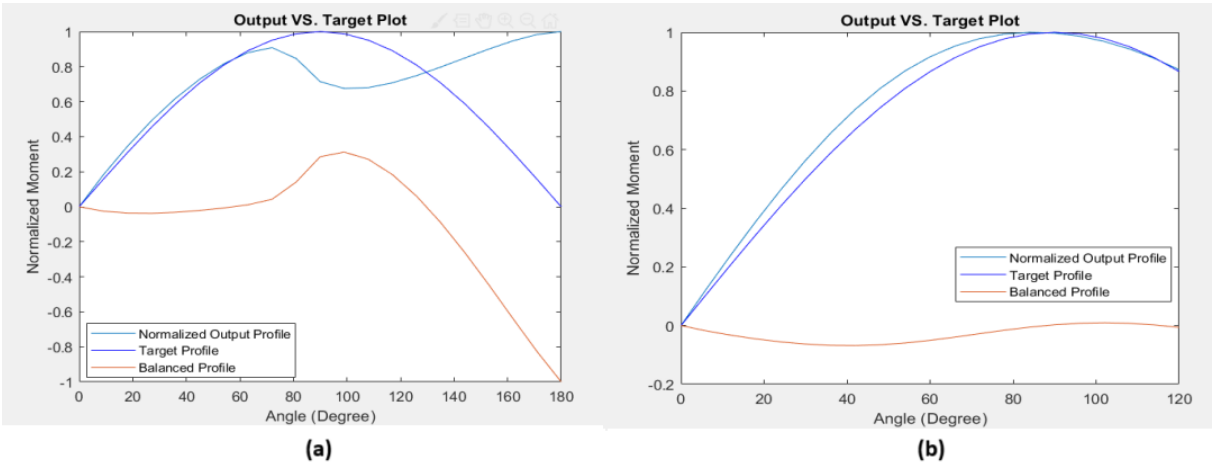

Figure C.8.: The optimized torque-angle profile for the L-shape helicoidal shell in the target window of 180 degrees that is based on the variation of a) length factor, b) length factor, and sharpness factor along the height.

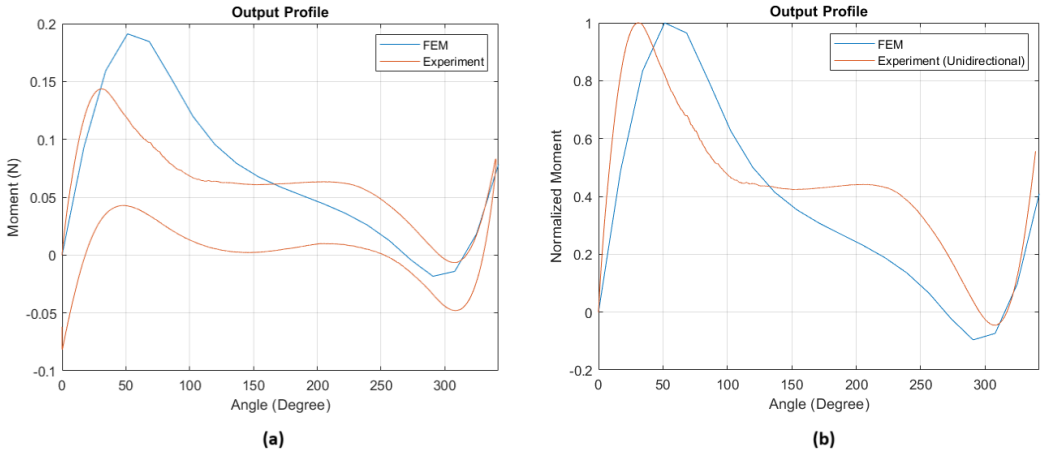

Figure C.9.: (a) Output profile of default L-shape prototype: FEM VS. experimental data and (b) Normalized moment

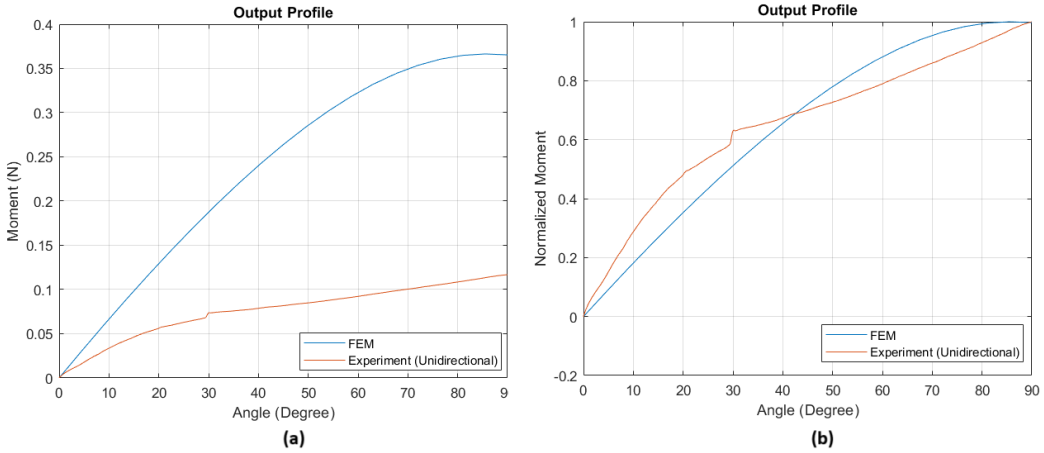

Figure C.10.: (a) Output profile of optimized L-shape prototype for 90 degrees: FEM VS. experimental data and (b) Normalized moment

D

Synthesis of Nonlinear Output Profiles: An Example

The main focus of this research was directed towards obtaining a gravity-balancing profile using variations of a helicoidal shell joint. However, in the grand scheme of things, the objective is to propose a tunable structure where a wide range of nonlinear torque-angle profiles can be achieved This appendix will address an example of a joint, studied by Hampali et. al. [1], which is designed for a particular nonlinear profile, and recreating this profile by optimizing the L-shape helicoidal joint. Hampali et. al. [1] have developed two variants of their design. Figure D.1 (a) and (b) show the undeformed and deformed shape of the first type of this joint respectively and Figure D.1 (c) and (d) show the undeformed and deformed shape of the second type of this joint respectively. Figure D.2 shows the target profile (a) envisioned profile and (b) implemented profile by Hamapali et. al. [1]. By using a normalized target function, we can attempt to recreate this profile by optimizing the L-shape helicoidal joint. Figure D.3 shows the optimized profile achieved by the L-shape helicoidal joint by using the methodology employed in this thesis. This result shows further tunability and potential of helicoidal shells for the synthesis of nonlinear torque-angle profiles. Figure D.4 shows the CAD model corresponding to this optimized joint.

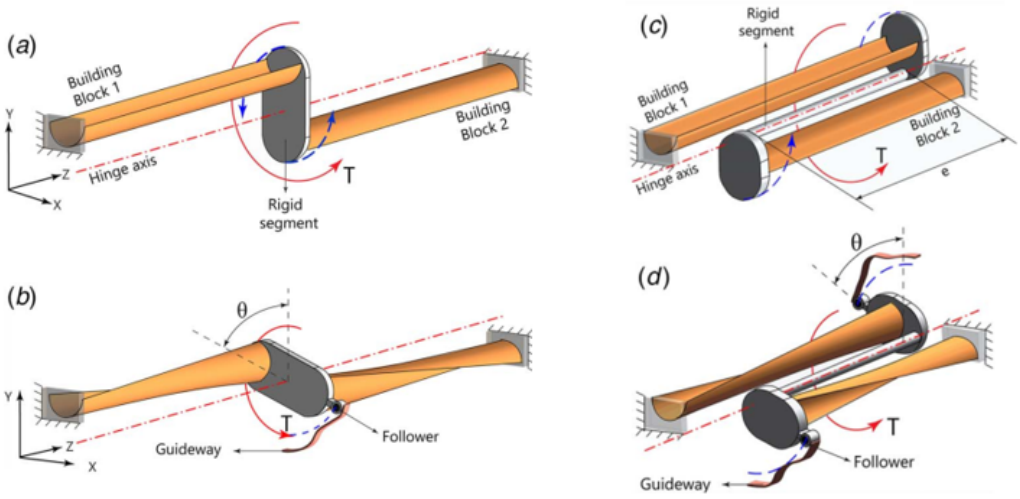

Figure D.1.: The compliant joint studied by Hampalt et. al. [1]

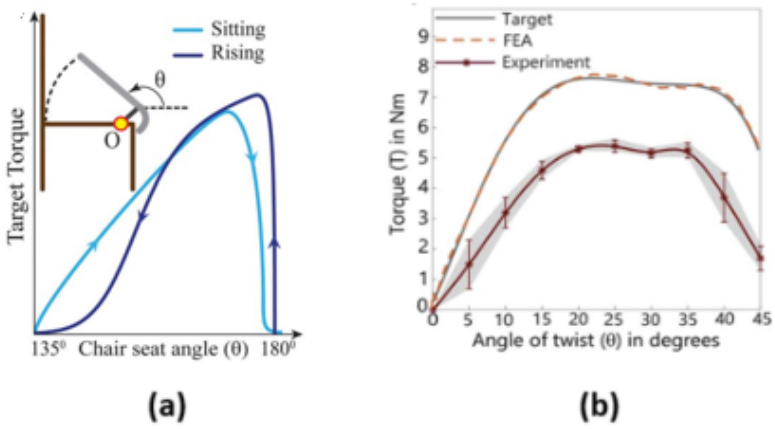

Figure D.2.: (a) Qualitative target profile b) Actual target profile (simulation and experiment.) [1]

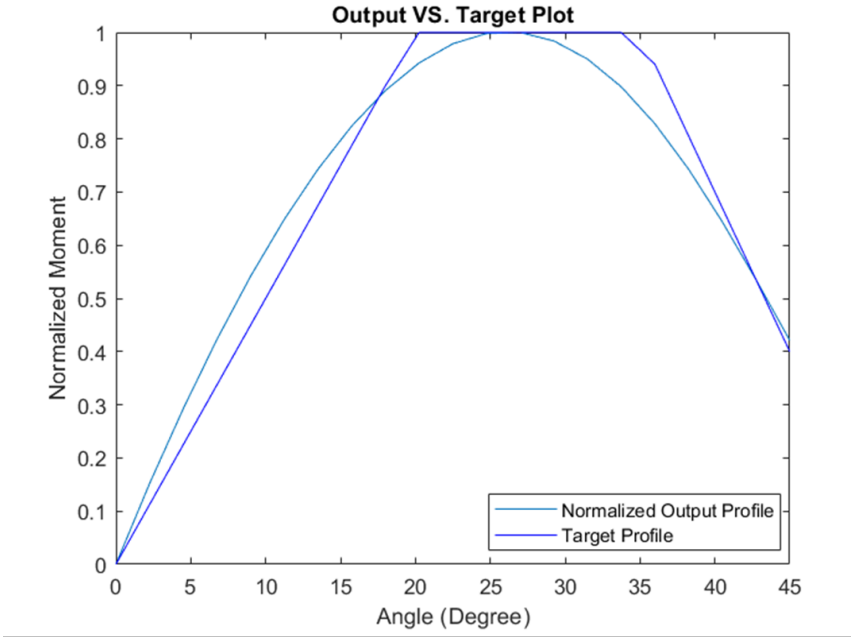

Figure D.3.: The recreated optimized profile bu using L-shape helicoidal joint

REFERENCES

[1] S. Hampali, A. P. S, and G. K. Ananthasuresh. "A Tunable Variable-Torque Compliant Hinge Using Open-Section Shells". In: *Journal of Mechanisms and Robotics* 12.6 (Dec. 2020). DOI: 10.1115/1.4047440.

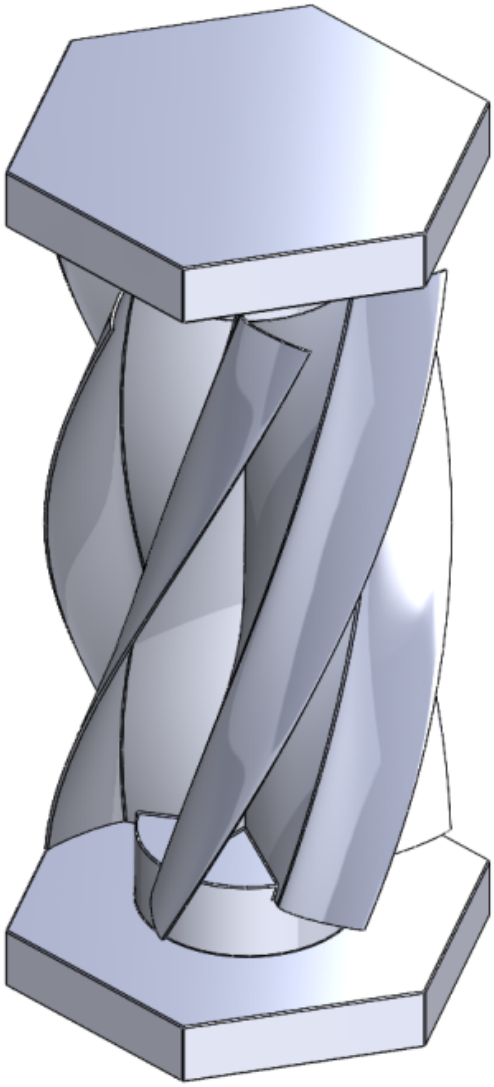

Figure D.4.: The CAD model for the optimized joint